10-30-2008

Developments Toward a Micro Bistable Aerial Platform: Analysis of the Quadrantal Bistable Mechanism

Aaron A. Muñoz
University of South Florida

DEVELOPMENTS TOWARD A MICRO BISTABLE AERIAL PLATFORM: ANALYSIS OF THE QUADRANTAL BISTABLE MECHANISM

by

Aaron A. Muñoz

A thesis submitted in partial fulfillment
of the requirements for the degree of
Master of Science in Mechanical Engineering
Department of Mechanical Engineering
College of Engineering
University of South Florida

Major Professor: Craig P. Lusk, Ph.D.
Autar K. Kaw, Ph.D.
Nathan B. Crane, Ph.D.

Date of Approval:
October 30, 2008

Keywords: microelectromechanical systems (MEMS), compliant, out-of-plane, ortho-planar, 3-D mechanism, pop-up structure, pseudo-rigid-body model

ACKNOWLEDGMENTS

I would like to express my utmost appreciation to Dr. Craig Lusk who gave me the opportunity to join in his research and to benefit from his wisdom. I would like to thank him for the guidance he has given me and for the many hours he spent on my behalf to ensure my success. I will always be grateful. Also, I would like to thank my graduate committee members, Dr. Nathan Crane and Dr. Autar Kaw, for their commitment to helping me improve this thesis. Furthermore, I would also like to thank my father who inspired me to become an engineer and to the rest of my family for their support throughout my education.

Additionally, I would like to thank the many people in the College of Engineering and the Mechanical Engineering Department at the University of South Florida that make this university great. This work was supported, in part, by the University of South Florida Office of Research & Innovation through the New Researcher Grant Program under Grant Number R057524.

Finally, I am thankful to my Heavenly Father for His love, care, and guidance through all the stages of my life, including this research.

TABLE OF CONTENTS

LIST OF FIGURES

DEVELOPMENTS TOWARD A MICRO BISTABLE AERIAL PLATFORM: ANALYSIS OF THE QUADRANTAL BISTABLE MECHANISM

Aaron A. Muñoz

ABSTRACT

The Bistable Aerial Platform (BAP) has been developed in order to further enlarge the repertoire of devices available at the microscale. This novel device functions as a switch in that its platform can lock in two positions, up or down. Herein, it will be examined and explained, but a true understanding of its workings requires a better understanding of its compliant constituent parts. The Helico-Kinematic Platform (HKP), which serves as an actuator for the BAP, is currently under investigation by another researcher and will be merely touched upon here. The focus, therefore, will rest on the analysis of the Quadrantal Bistable Mechanism (QBM), the principle component of the BAP. A preliminary pseudo-rigid-body model, an aid for the understanding of compliant mechanisms, will also be examined for the QBM. The models developed for these two devices, the HKP and QBM, can later be combined to form a full model of the Bistable Aerial Platform.

CHAPTER 1: INTRODUCTION

At the microscale, compliant mechanisms are of vital importance because "frictional forces encountered in conventional rigid joints dominate [the inertial forces] at micro level, thus making the use of rigid-link mechanisms inappropriate for micro applications" [1]. Because friction in the microscale discourages the use of gears and joints due to excessive energy loss, the obvious alternative choice is compliant mechanisms since they do not suffer frictional losses [2]. A study of compliance is of particular importance to the further development of microelectromechanical systems (MEMS) because compliant mechanisms reduce part counts when compared with rigid-body mechanisms that produce the same function, thus enabling further miniaturization. However, due to their use of large, nonlinear deflections, their analysis proves far more demanding than an equivalent rigid-body mechanism. For this reason, Pseudo-Rigid-Body Models (PRBMs) are developed, easing the analysis of new compliant mechanisms, allowing them to be modeled by an equivalent rigid-body mechanism [3].

1.1. Objective

The purpose of this research is to describe a novel compliant mechanism, the Bistable Aerial Platform (BAP), and to begin the development of a pseudo-rigid-body model. Towards this end, a preliminary PRBM was examined for a critical component of the BAP, the Quadrantal Bistable Mechanism (QBM). A finite element analysis (FEA) of both the QBM and BAP was also done (See Appendices for ANSYS code). A full PRBM of the BAP will be possible when complimentary research on the Helico-Kinematic

Platform (HKP), another key component that functions as an actuator for the BAP, is completed.

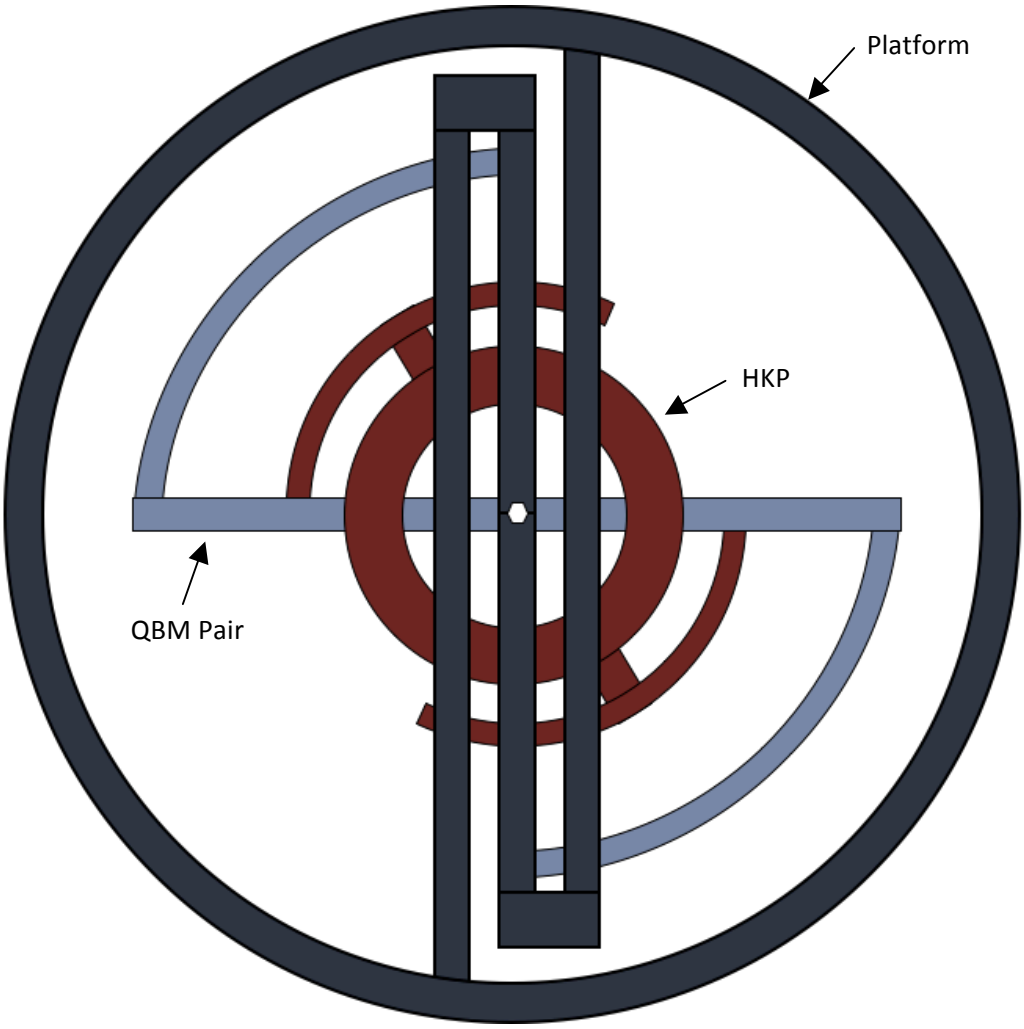

Figure 1.1 Illustration of the Bistable Aerial Platform

1.2. Motivation

The Bistable Aerial Platform is a compliant mechanism that converts a rotational input into a large ortho-planar displacement of a platform with two stable equilibrium positions (down and up). At the micro level, it is unique in that it is the first MEMS platform that can maintain either its up or down position without a constant input force

due to bistability. Additionally, the platform itself is among the largest surface micro-machined surfaces to be raised out-of-plane. For these reasons, the device may have applications in micro optics as mirrored platform in DLP projectors, in tactile displays as a controlled array of Braille dots, or as an integrated micro-antenna that uses the raised platform ring for RF signals.

1.3. Scope

The Bistable Aerial Platform is formed from the combination of two compliant mechanisms as well an additional rigid-body mechanism. Equations describing the motions of the rigid-body components of the BAP are easily derived, but the analysis required for the compliant components is much more involved. The pseudo-rigid-body model of the Helico-Kinematic Platform [4] is currently under development by another researcher and thus lies outside the scope of this research. This paper will therefore focus on the Quadrantal Bistable Mechanism, a device closely related to that studied by León et al. [5]. This research improves upon the existing PRBM, which provides equations for beam deflection, by incorporating elastic deformation of the beam into the model. With the proper pseudo-rigid-body models for both the QBM and HKP, the Bistable Aerial Platform will become easier to study and explain.

1.4. Contributions

The primary contribution of this research is the integration of the Quadrantal Bistable Mechanism and Helico-Kinematic Platform to form the Bistable Aerial Platform, based upon the recognition that the leg of a HKP can function as a dual output device. Subsequent contributions involved detailed analyses of the QBM with the aim of successfully prototyping the BAP. First, a finite element analysis was performed on the

BAP and two finite element analyses were done on the QBM. One FEA of the QBM was done to confirm that this application within the BAP correlated to that done by León et al.[5]; the other FEA was used to gather data on the elastic deformation experienced by the QBM. To analyze the FEA data, MATLAB code was produced and used to improve the related pseudo-rigid-body model developed by León et al. [5].

1.5. Research Approach

All information presented up to this point has served to introduce the subject matter of this thesis. In the next chapter, the relevant background information needed to better understand later portions of this thesis will be presented. Following that, this paper will follow the actual research approach undertaken. Chapter Three will describe the Bistable Aerial Platform and how it was developed. Then, in the next chapter, the MEMS prototype of this device will be examined.

Following this, the focus will shift to the QBM. Chapter Five will explain a force relationship for the QBM that is crucial to the operation of the BAP. Then in Chapter Six, a preliminary PRBM of a spherical fixed-guided beam, which corresponds to the QBM, will be introduced and analyzed. Finally, in Chapter Seven, the overall BAP design will be discussed and the results concerning the PRBM will be summarized.

CHAPTER 2: BACKGROUND

2.1. MEMS

The current push for miniaturization, as witnessed in electronics as the quest for the ever-smaller microprocessor, has recently spawned a novel field of micro machines, better known as microelectromechanical systems (MEMS), which are continually becoming more commonplace as additional technologies and applications continue to develop. Micromanufacturing, as a technology, is relatively new; it was begun in the mid 1960's [6] and did not branch off into the MEMS process until 1987 [2]. In its few scant decades of existence, microelectromechanical systems development has come a long way.

The fabrication approach of MEMS is one that conveys the advantages of miniaturization, multiplicity, and microelectronics to the design and construction of integrated electromechanical systems [2][7]. Miniaturization is of course an inherent aspect of MEMS as is implied by its name; and, with batch processes such as surface micromachining now allowing many mechanisms to be made for the same cost as a single device, multiplicity can really come into play for MEMS. This is important because it enables an array of single devices to produce macroscale effects that would be impossible for a discrete device [8]. Additionally, the MEMS process makes use of the same fabrication techniques and materials used for microelectronics, which enables the integration of both mechanical and electrical components [7].

2.2. Compliant Mechanisms

Compliant mechanisms are devices that gain their mobility from elastic deformation rather than the rigid-body motions of conventional mechanisms [9][10]. Unlike traditional rigid-link mechanisms where elastic deformation is detrimental to performance, a compliant mechanism is designed to take advantage of the flexibility of the material [11]. The function of the compliant member within a compliant mechanism can be as basic as serving as a simple spring or as complex as generating a specified motion [12]. The fully-compliant mechanism uses flexible structures to emulate the overall performance of rigid-link mechanisms with without any rigid joints whatsoever [13].

Compliant mechanisms are well suited for MEMS applications because their joint-less, single-piece construction is unaffected by many of the difficulties associated with MEMS, such as wear, friction, inaccuracies due to backlash, noise, and clearance problems associated with the pin joints [13]. In addition, compliant mechanisms are planar in nature, do not require assembly, and can be made using a single layer [13]. This greatly enhances the manufacturability of micromechanisms because MEMS are planar and are typically built in batch production with minimal or no assembly [1].

2.3. Pseudo-Rigid-Body Model

A simple, accurate method for modeling compliant mechanisms is the pseudo-rigid-body model. This model functions by replacing flexible members with conventional kinematic members; thus, allowing the designer to model the compliant mechanism using rigid-body equations [3]. Most, but not all, of the typical configurations of flexible segments can be analyzed using this method.

When an element bends, its ends follow a certain path. Therefore, what the pseudo-rigid-body model does is attempt to accurately model the behavior of a compliant mechanism by replacing a flexible segment with rigid segments and pin joints at optimized locations that will allow the end to follow the same deflection path. The stiffness of the flexible segment is balanced by the addition of torsional springs because, "unlike rigid-body mechanisms, energy is not conserved between the input and output port of compliant mechanisms because of energy storage in the flexible members" [14].

2.3.1. Fixed-Free Flexible Cantilever

As an example of the pseudo-rigid-body model, the flexible cantilever beam will be examined as it is one of the more common applications of the PRBM. A flexible cantilever beam with a constant cross section is shown in Figure 2.1(a) [15]. Note that the application of a force orthogonal to the beam at the free end will cause the end of the beam to deflect and follow a nearly circular path. The PRBM assumes that this nearly circular path can be modeled by two beams that are pinned together forming a pivot. This *characteristic pivot* is positioned a fractional distance γl from the free end of the beam where γ is the *characteristic radius factor* of the length, l. Thus making γl the *characteristic radius* that represents the length of the pseudo-rigid-body link and radius of the circular deflection path it travels [15]. In order to incorporate the beam's resistance to deflection into the model, a torsional spring is added at the characteristic pivot. The resulting pseudo-rigid-body model, shown in Figure 2.1(b), will have approximately the same deflection path and vertical force response as the original compliant structure.

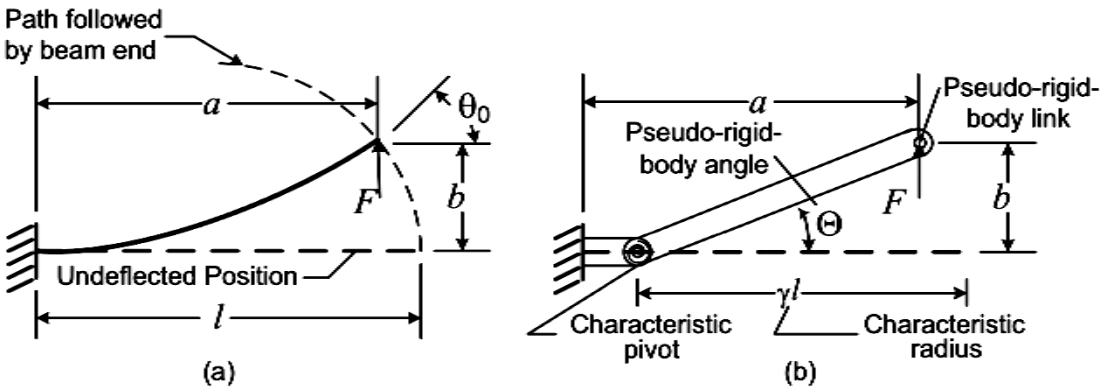

Figure 2.1 **(a)** Cantilever with a vertical force at the free end
(b) Equivalent pseudo-rigid-body model
[5][1]

2.3.2. Fixed-Guided Flexible Beam

The PRBM for the fixed-guided flexible beam is closely related to the fixed-free flexible cantilever. The difference is that the angle of the "guided" end does not change, which requires a moment, M_o, be present at the guided end [15]. This causes the deflected shape of the beam to be antisymmetrical at its centerline as shown in Figure 2.2(a). Note that the midpoint has zero curvature, which implies that the moment at the midpoint of the beam is also zero because moments are directly proportional to the curvature, per the Bernoulli–Euler equation [15]. Without a moment at the midpoint, the free-body diagram for one-half of the beam is as shown in Figure 2.2(b), which matches the flexible cantilever. Thus, the PRBM for half of the fixed-guided beam will be the same as the PRBM for the fixed-free beam. Therefore, combining two antisymmetric one-half beams, as shown in Figure 2.2(c), will form the PRBM for the entire beam and ensure that no moment is created at the center [15].

[1] Image used with permission.

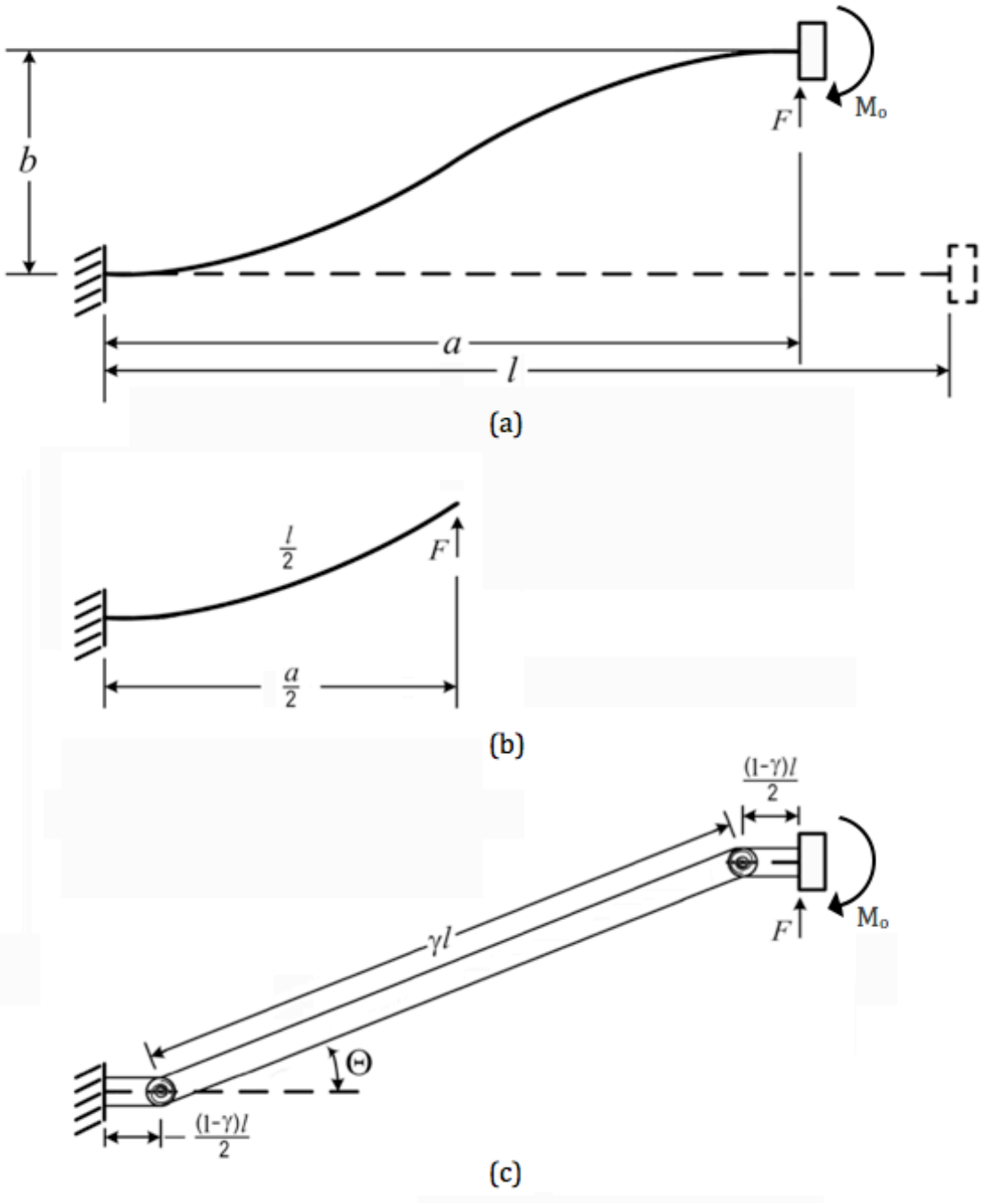

Figure 2.2 **(a)** Fixed-guided flexible beam **(b)** Free-body diagram of one-half of the beam **(c)** Pseudo-rigid-body model
[15][2]

[2] Image adapted from Howell

2.4. Bistability

A system is considered to be stable if a small external disturbance only causes it to oscillate about its current position. The position is unstable if that same disturbance causes the system to move to another position [15]. An example of these states is shown below in Figure 2.3.

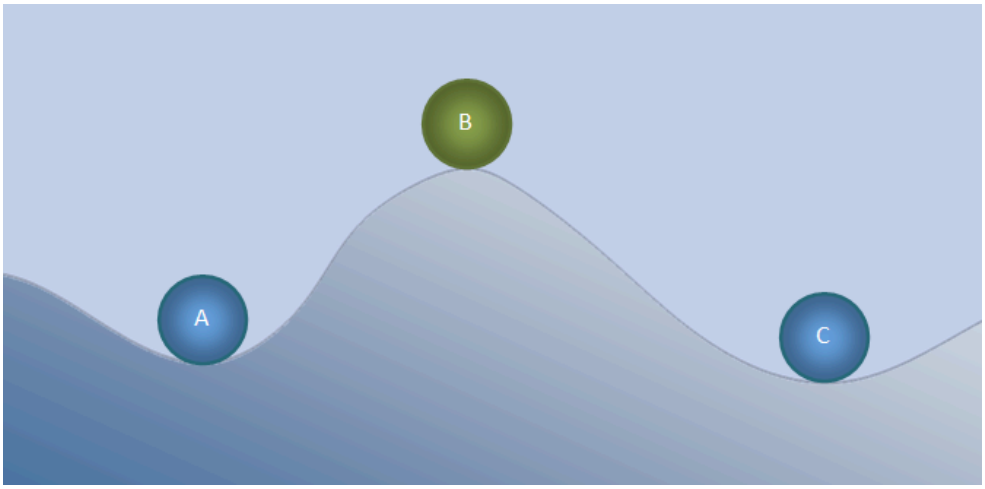

Figure 2.3 The "ball-on-the-hill" analogy.
Positions A and C are stable positions. Position B is unstable.
[15][3]

Typical mechanisms are monostable, having only one stable state, and require a sustained force in order to hold a second stable state [16]. A bistable mechanism, on the other hand, is capable of holding one of two stable states at any given time, and consumes energy only during the motion from one stable state to the other [16]. This bistable behavior is achieved "by storing energy during part of its motion, and then releasing it as the mechanism moves toward a second stable state" [17]. Because flexible segments store

[3] Image adapted from Howell

energy as they deflect, compliant mechanisms can be designed to use the same segments to gain both motion and a second stable state, which results in a significant reduction in part count [17].

2.5. Spherical Mechanisms

In planar mechanisms, the joint axes are parallel to each other and normal to the plane in which the mechanism undergoes its motion. In spherical mechanisms, however, the joint axes all intersect at the center of a sphere which causes each link to rotate about this fixed point in space [4][18]. A spherical mechanism therefore requires that the axes of all joints fixed in space to the ground (or reference) link intersect at a common point. Additionally, mobile joint axes not connected to ground, which change their orientation in space, must be constrained by their linkage geometry to pass through that same center point [4]. The Quadrantal Bistable Mechanism and the Helico-Kinematic Platform, which form the Bistable Aerial Platform, are both spherical mechanisms. Therefore, the BAP itself is a partial spherical mechanism in which most of the joint axes rotate about the mechanism's center.

CHAPTER 3: BISTABLE AERIAL PLATFORM

3.1. Compliant Components

In order to understand the BAP, it is necessary to describe its mechanical components. This mechanism is comprised of three building-block elements. The first element is a Quadrantal Bistable Mechanism (QBM), which is the cornerstone of the BAP and closely relates to a simplified spherical PRBM developed at USF [19][20]. The second is a compliant Helico-Kinematic Platform [4] that serves to actuate the QBM. The final element is a variation of the scissor lift mechanism that attaches to the output of the QBM and amplifies the ortho-planar displacement.

3.1.1. Quadrantal Bistable Mechanism

The Quadrantal Bistable Mechanism consists of two links that rotate about intersecting, orthogonal axes. The rotation of one link (the *planar link*) is in-plane while the other (the *ortho-planar link*) rotates out-of-plane. The axes of rotation of the planar and ortho-planar links are called the *planar axis* and *ortho-planar axis*, respectively. In the QBM's initial position, the links are perpendicular to each other and lie in (or near) a common base plane. A thin, compliant beam, the *quadrantal beam*, connects the two links and forms an arc that is approximately a quarter circle (or quadrant). See Figure 3.1 and Figure 3.2.

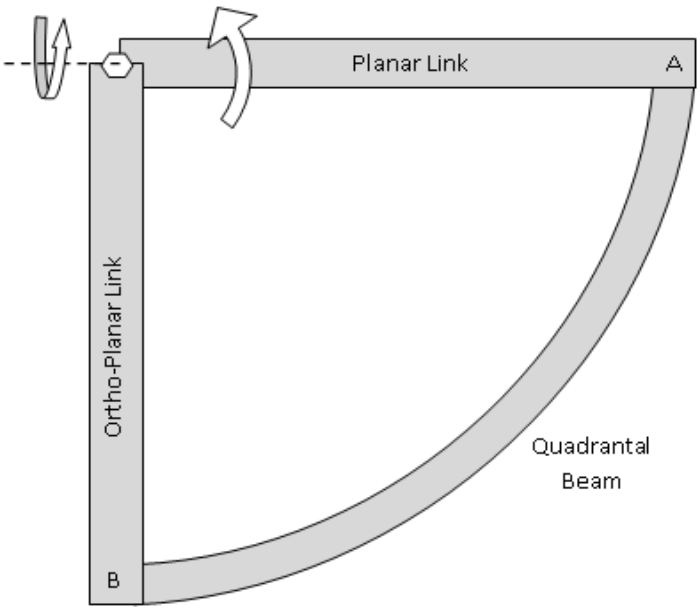

Figure 3.1 Top view of Quadrantal Bistable Mechanism

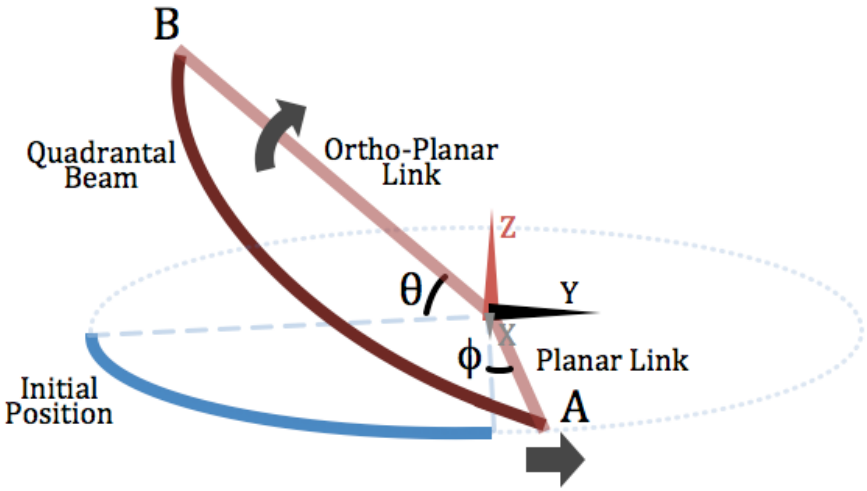

Figure 3.2 Side view of Quadrantal Bistable Mechanism

There are two potential input links for the QBM. Either the planar or the ortho-planar (OP) link may be used either individually or simultaneously. Regardless of the mode of actuation, the mechanism can move from its initial (first stable) position to its second stable position, which occurs when the ortho-planar link reaches ninety degrees of rotation.

Equations defining the QBM's position have already been developed for the case where the driving link rotates out-of-plane [20], but work has yet to be done for the case of the planar driving link. This is partly because a relatively large force, the *planar threshold force*, is required to actuate the mechanism using the planar link. The benefit of actuating the device in this manner, however, is that with only a few degrees of rotation, the ortho-planar link is drawn through a full ninety degrees into its second stable position. Fortunately, providing a bias to the mechanism by first raising the ortho-planar link greatly reduces the planar threshold force. The higher the ortho-planar link is raised, the less force is needed to rotate the planar link; this force phenomenon will be further examined in chapter five.

3.1.2. Compliant Helico-Kinematic Platform

The compliant Helico-Kinematic Platform (HKP) is a spherical mechanism in which a platform is raised out-of-plane by the coordinated buckling of beams. Shown in Figure 3.3 is a long, thin beam fixed at one end and with the motion of its other end limited by a longitudinal slide. Upon applying a longitudinal, compressive force to the beam at the slide, the beam will buckle and displace its center. By taking two or more of

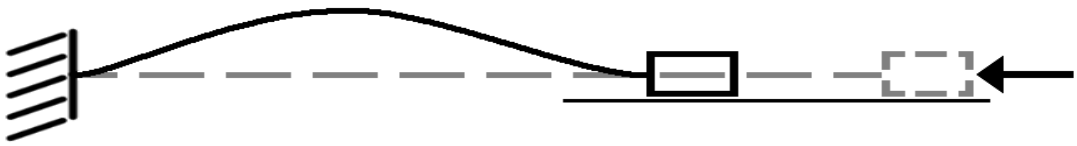

Figure 3.3 Linear beam buckled under a compressive load

these beams and attaching a common platform at their centers, their displacements will be constrained such that the beams will only buckle out-of-plane, thus raising the platform. Curving these beams around a circular platform will allow these them to be

simultaneously actuated by a single rotary input (See Figure 3.4). When buckled, these beams, *legs*, support the HKP like the legs of a table (See Figure 3.5).

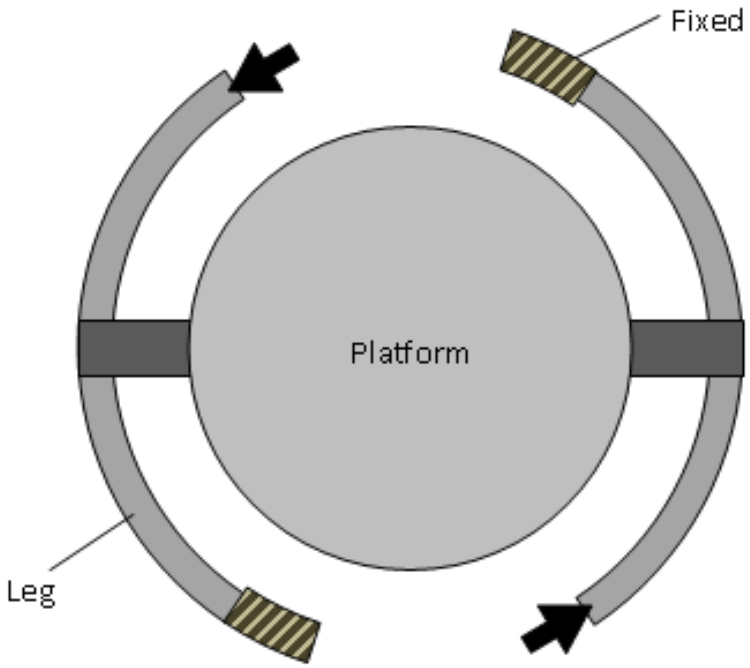

Figure 3.4 Top view of Helico-Kinematic Platform

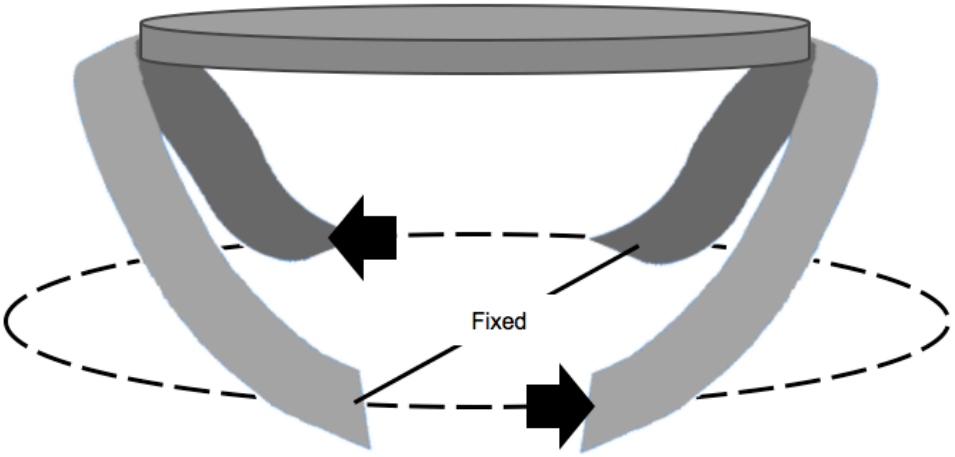

Figure 3.5 Side view of actuated HKP

3.2. Inception of the Bistable Aerial Platform

The Bistable Aerial Platform resulted from probative examinations of the Quadrantal Bistable Mechanism. Of particular note was the behavioral response using the planar link as the input. A decreasing planar threshold force was obtained by biasing the ortho-planar link with an initial ortho-planar displacement (See Figure 3.6). The observation of this phenomenon later led to the inspiration to use of the HKP as a means of providing input simultaneously to both the planar and the ortho-planar links.

Figure 3.6 Planar threshold force vs. θ

3.2.1. QBM Pair

The continued investigation into the QBM was done with the objective of developing a new mechanism utilizing the QBM to provide bistability to some platform-

type mechanism. The initial thought was to use multiple QBMs positioned around the platform and have the many ortho-planar links raise the platform. While this would make for a very stable platform, the concept was abandoned due to the challenges involved in simultaneously actuating separate QBMs. The chosen alternative was to make use of the spherical design of the QBM and merge two QBMs into a unified mechanism that share the same base plane, planar axis, ortho-planar axis, and center point. To achieve this, one QBM was rotated by one hundred eighty degrees with respect to the other about their common planar axis (See Figure 3.7). With the planar links further conjoined, only a single rotary input will be needed to simultaneously actuate both QBMs.

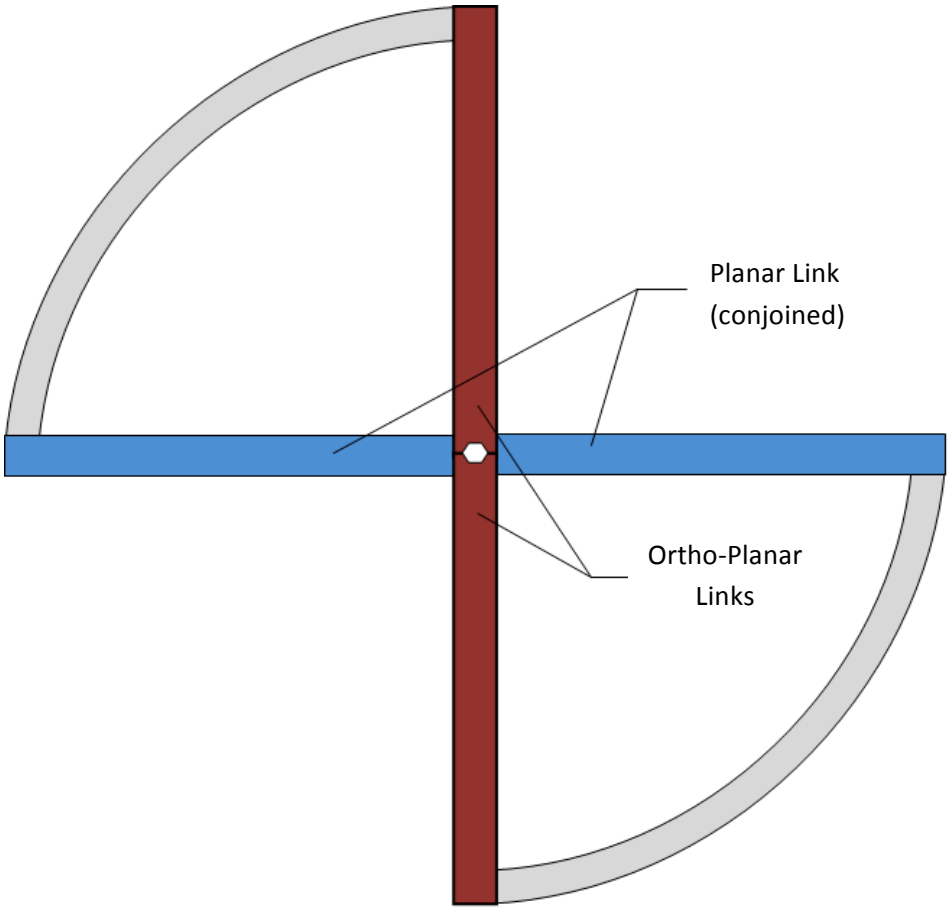

Figure 3.7 Conjoined QBM Pair

3.2.2. HKP Actuation

Actuation is accomplished through the use of a compliant Helico-Kinematic Platform. Recall that the legs of the compliant HKP must be compressed in order to buckle and that the simplest way to accomplish this is for one end to be fixed while a compressive force is applied to the other end. Also recall that the QBM, when actuated by rotating the planar link, without an out-of-plane bias of the ortho-planar link, requires a very large planar threshold force to initiate movement. Therefore, the planar link is virtually fixed until the planar threshold force is reached, thereby allowing the attachment of the "fixed" end of a HKP leg to the planar link.

In the BAP, the HKP acts as a transmission to provide input forces to the two QBMs. The beauty of using this mechanism for actuation is that it can provide the planar threshold force and raise the ortho-planar links to give the needed bias. This is accomplished by situating the HKP, a spherical mechanism requiring rotary input, concentric with the QBMs. Its platform is cut to form an annulus and designated as the *elevating ring*. From this location (See Figure 3.8), the elevating ring can concurrently raise the ortho-planar links of both QBMs in order to reduce the planar threshold force. Thus, when the HKP is rotated, its compliant legs are compressed by the "fixed" planar links and therefore buckle. This forces the elevating ring to rise and lift the QBMs' ortho-planar links (See Figure 3.9). The elevating ring and ortho-planar links will continue to rise until the planar threshold force decreases sufficiently to equal the force required to buckle the legs. When this occurs, the QBMs' planar links rotate causing the ortho-planar links to be drawn upright and the elevating ring to suddenly collapse as its supports un-

buckle due to the withdrawal of the compressive force needed to maintain it in the raised position. These forces are explained further in Chapter Five.

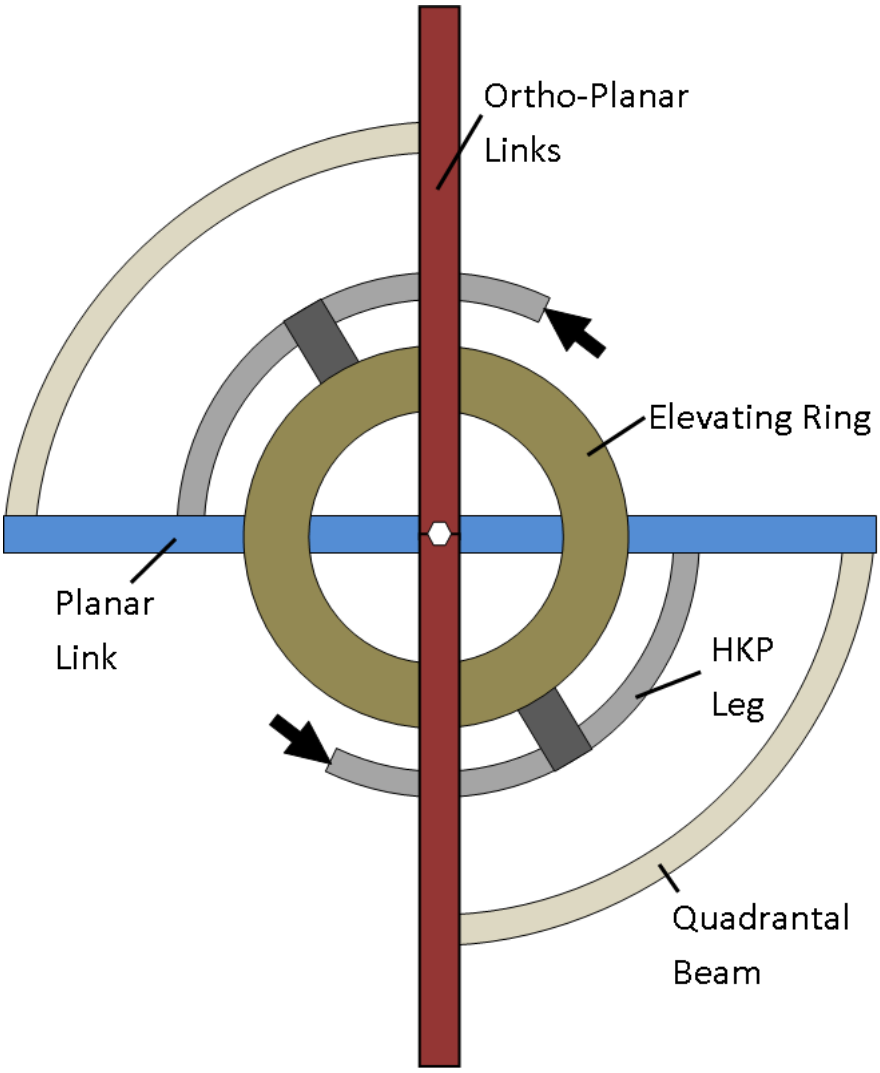

Figure 3.8 Integrated compliant components of the BAP

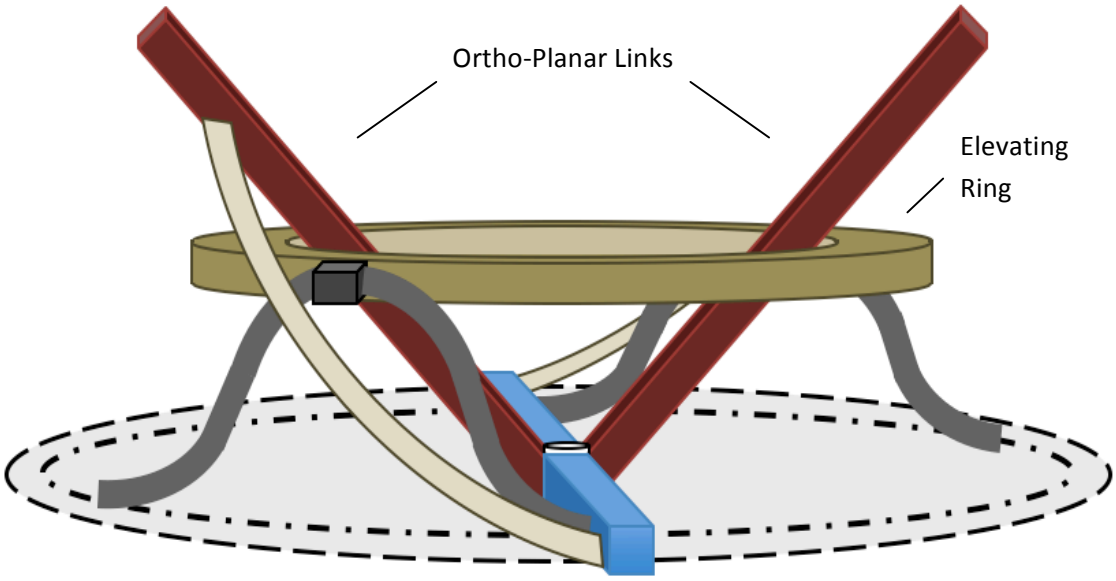

Figure 3.9 Elevating ring lifting the ortho-planar links

When the QBMs' links are upright, the QBMs are in their second stable position. Thus, the BAP is in its second stable position requiring no additional forces to maintain itself. Because this position is stable, the QBM's ortho-planar links will resist forces smaller than the *ortho-planar threshold force*. Similar to the case for the planar threshold force, the magnitude of the ortho-planar threshold force will depend on the position of the QBM's planar link.

The compliant HKP again proves ideal because it can also de-actuate the BAP. A simple reversal in the direction of the input forces on the HKP will put the legs under tension and pull the attached planar links of the QBMs. Once the planar links reach their initial positions, the ortho-planar links simply fall back down. Throughout this deactivation, the elevating ring will remain down.

3.2.3. Platform Integration

The integral bistable mechanism of the Bistable Aerial Platform and its method of actuation have been described; all that remains is to attach the actual platform. Note, the elevating ring of the compliant HKP is not bistable nor does it lock in the up position. The "bistable platform" of the BAP is a separate, additional platform that is connected to the ends of the two ortho-planar links, as they are the only links that lock in the second stable position.

As the BAP actuates, the ortho-planar links of the QBM pair form a V-shape whose interior angle becomes increasingly more acute. This provides the required input motion for a scissor-lift mechanism. Connecting a traversing link to the ends of the ortho-planar links and pinning them at their centers would form the elongating crossing pattern of a scissor-lift as the device was actuated. However, in the fully actuated position this would provide merely a taller spike rather than the needed mount for a platform. Therefore, rather than pin the new links in the center in the traditional fashion of a scissor-lift, the links will instead be joined at their ends by means of a large ring to serve as a platform (See Figure 3.10). Connected in this manner, the new links now have a shifting "pivot" point that allows them to conform to a platform rather than coming together at the center (See Figure 3.11). The result is similar to that of the sliders used at the end of a scissor-lift in typical aerial platforms.

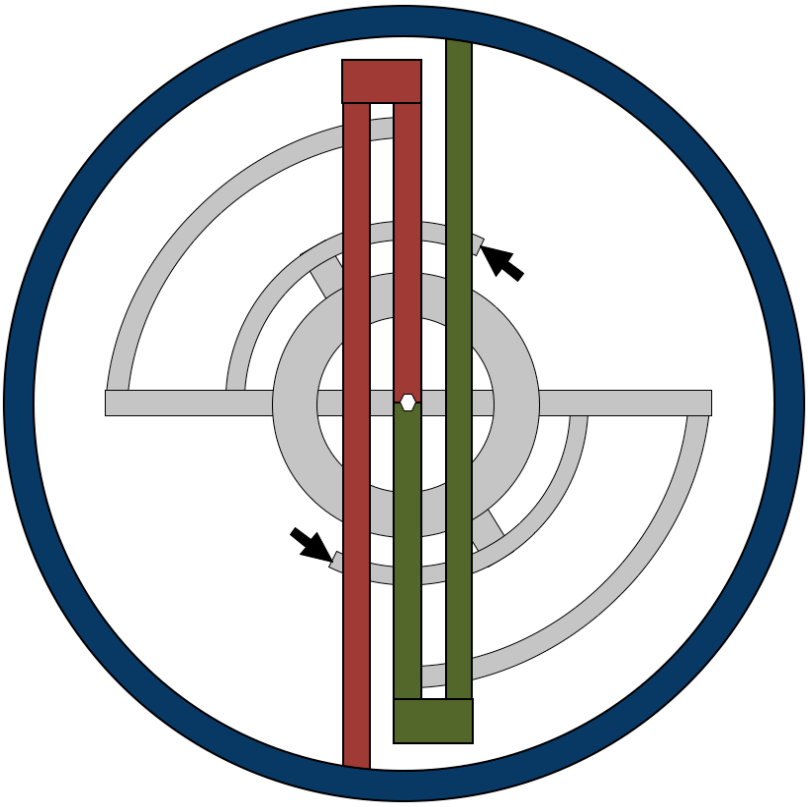

Figure 3.10 Top view of complete BAP mechanism showing the attached platform

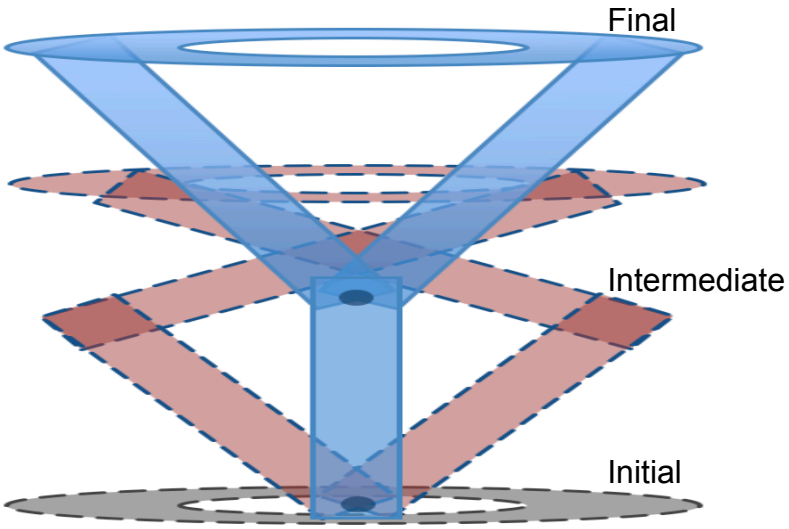

Figure 3.11 Side view of the BAP platform in its initial, intermediate, & final positions

CHAPTER 4: MICRO BISTABLE AERIAL PLATFORM

4.1. MEMS Prototype

The Bistable Aerial Platform was developed for possible micro applications in micro optics, tactile displays, or as a micro-antenna. This two-position device, if built at the macroscale, would prove overly complex and impractical compared to an equivalent mechanism. At the microscale, however this device is ideal because it is essentially flat and achieves its two positions with few mechanical parts, thus reducing friction.

The BAP prototype was built using the Multi User MEMS Process (MUMPs), one of the more common surface micromachining methods used in the microfabrication of MEMS, which introduces the following constraints to the design [16][21]:

1. a maximum of 3 polysilicon layers built on top of a silicon substrate
2. a limited ability to create a design that involves sliding the topmost layer of polysilicon over the lower layer, due to the natural conformation of the top layer over the lower polysilicon layer during the fabrication process
3. an inability to create a design that involves structures with large moving surface areas (unanchored to the ground substrate layer), due to the likelihood that the structure will be carried away in the fabrication process
4. a minimum surface feature of 2 μm
5. a minimum surface feature spacing of 2 μm

Shown in Figure 4.1 and Figure 4.2 are the design files for two variations of the BAP that conform to these constraints – units are in micrometers (μm).

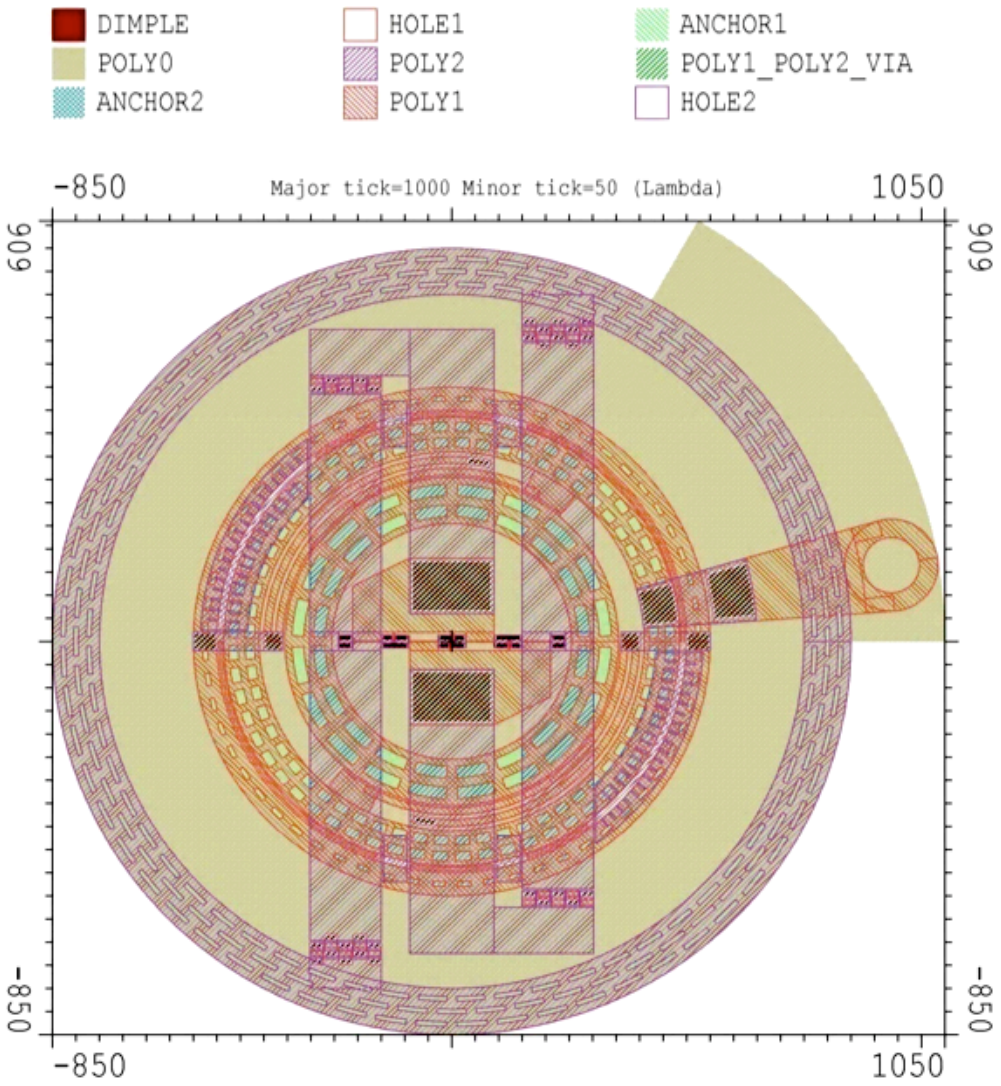

Figure 4.1 L-Edit design file of a Bistable Aerial Platform

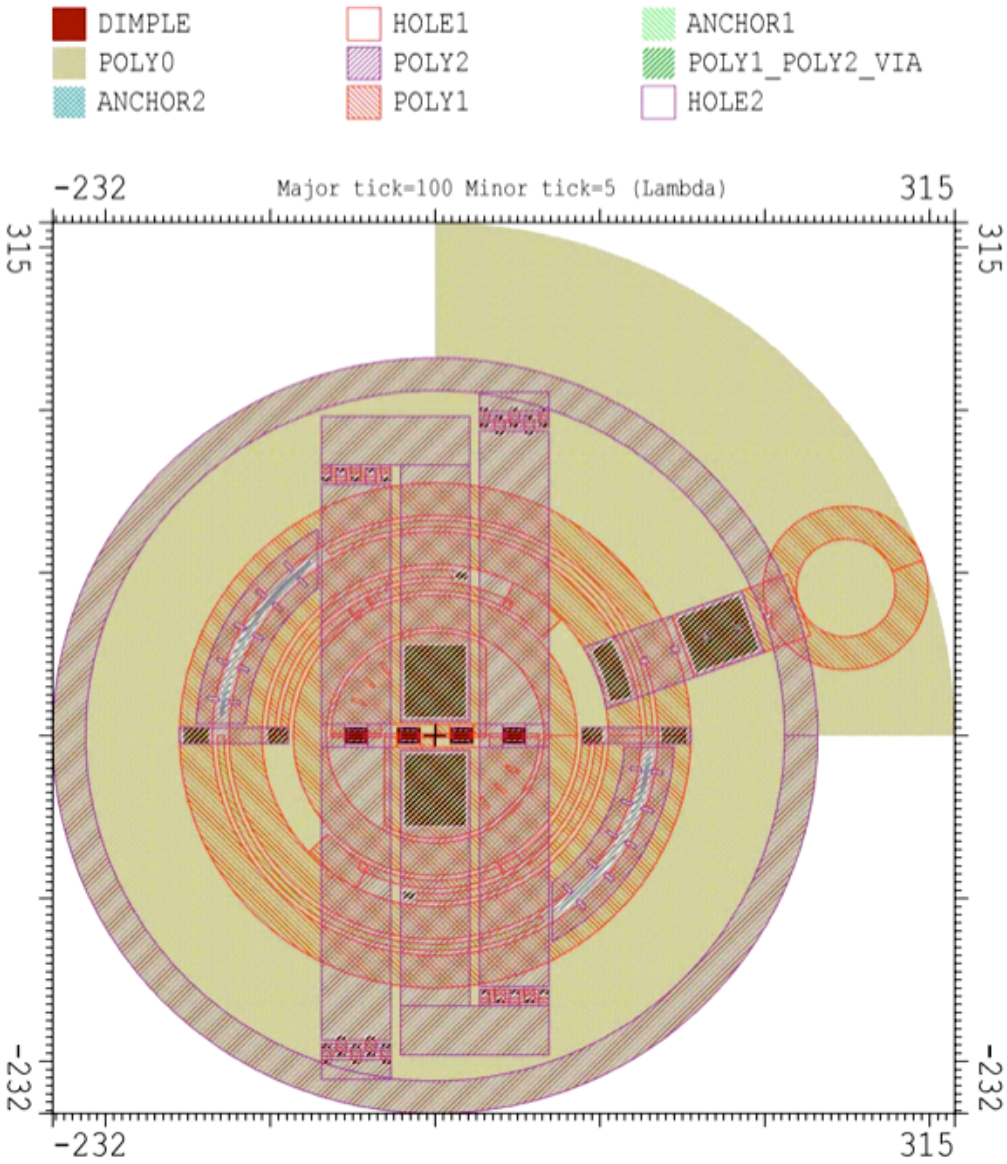

Figure 4.2 L-Edit design file of the small BAP variation

With just three structural layers, only two of which are capable of making movable components, portions of the device had to be moved radially outwards because they could not be accommodated in their ideal location. Such was the case for the planar links of the QBMs that must rotate together but cannot be connected and pinned at the center due to interference from the hinges for the ortho-planar links. Because the staple hinges used for the ortho-planar links require both moveable layers (See Figure 4.3: the

first movable layer is held down by the second), pinning the planar links could not also be done at the same location. This issue was resolved by limiting the planar links' motion to planar rotation by means of a guided, external ring (See Figure 4.4).

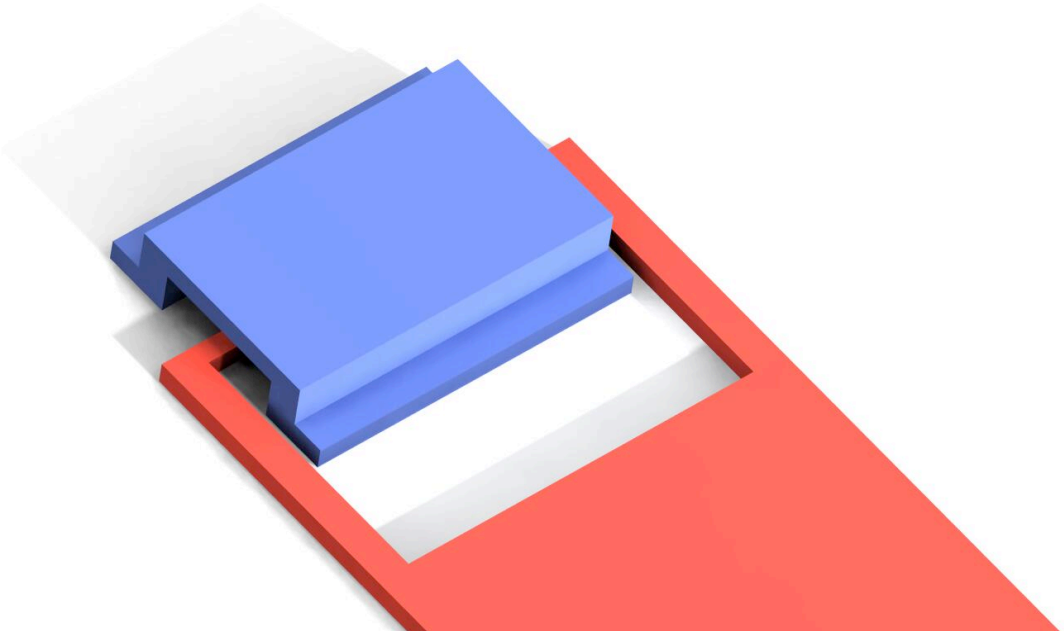

Figure 4.3 Typical MEMS staple hinge

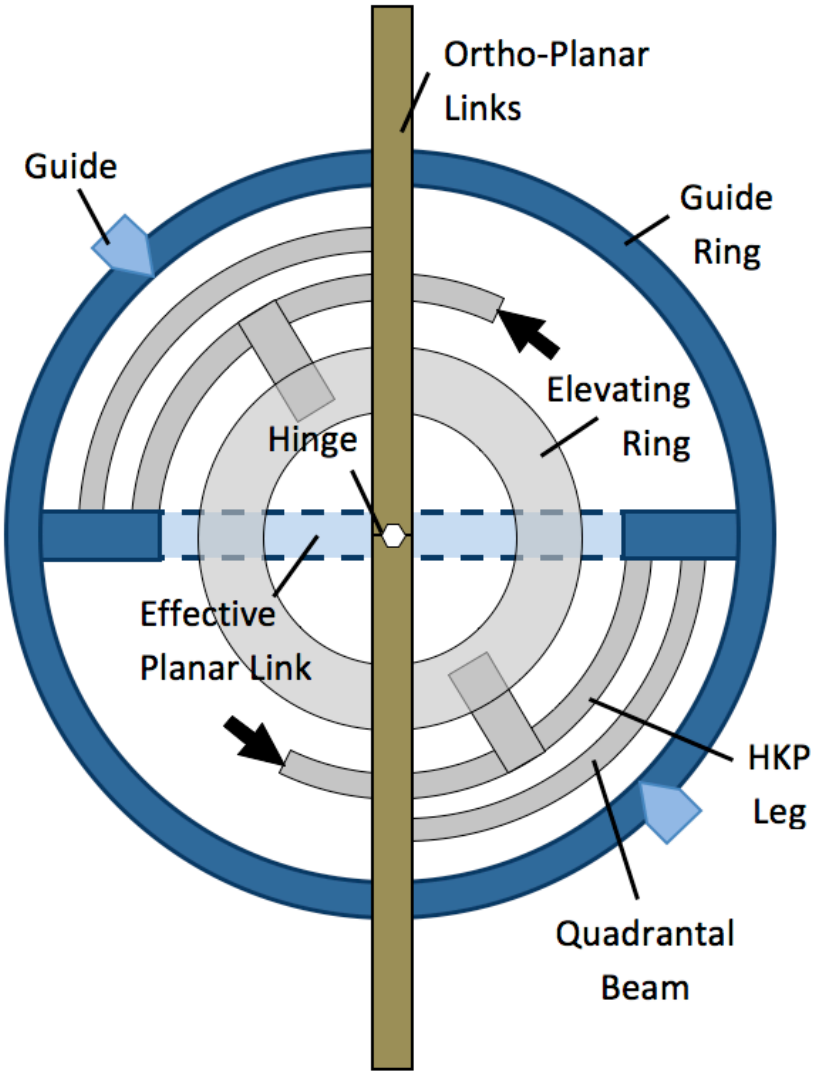

Figure 4.4 Micro BAP mechanism with guide ring

4.2. Die Release

Both variations of the BAP device were fabricated by MEMSCAP using their PolyMUMPS process. The completed dies arrived covered with a final protective layer of photoresist and with the various silicon dioxide, sacrificial layers produced during the manufacturing still in place. These sacrificial layers secure all the loose components during transit and protect the more fragile components. Completed MEMS devices must therefore be "released" by immersing them in a bath of hydrofluoric acid in order to

dissolve the sacrificial layers and free the structural members. This is followed by several minutes in deionized water and then alcohol in order to clear away residual acid. These steps must be done with precision to prevent pieces of the device being washed away. The die is then subsequently heated in an oven to reduce stiction.

The term stiction refers to the adhesion of the microstructure to adjacent surfaces [22]. Typically, it occurs after release as "freed" members become stuck to the newly exposed surface underneath the sacrificial layer [22][23]. Stiction becomes a vital issue in MEMS devices that incorporate large-area, very thin, compliant members with a small offset from adjacent surfaces [22][23]. If the strength of the adhesive bonding resulting from this contact exceeds the vertical pull-off force that can be generated by the structures, it will remain permanently stuck and be virtually anchored to the substrate [22][24]. The approach used to reduce or prevent stiction was to minimize the real area of contact through the formation of microscale standoff bumps ("dimples") on one surface, which increases the nominal separation between the surfaces [24][25].

Shown below in Figure 4.5 is a released Bistable Aerial Platform viewed through an optical microscope. In Figure 4.6 the smaller variation of the BAP is shown as observed through a scanning electron microscope (SEM). A released QBM, also viewed by a SEM, is shown in Figure 4.7.

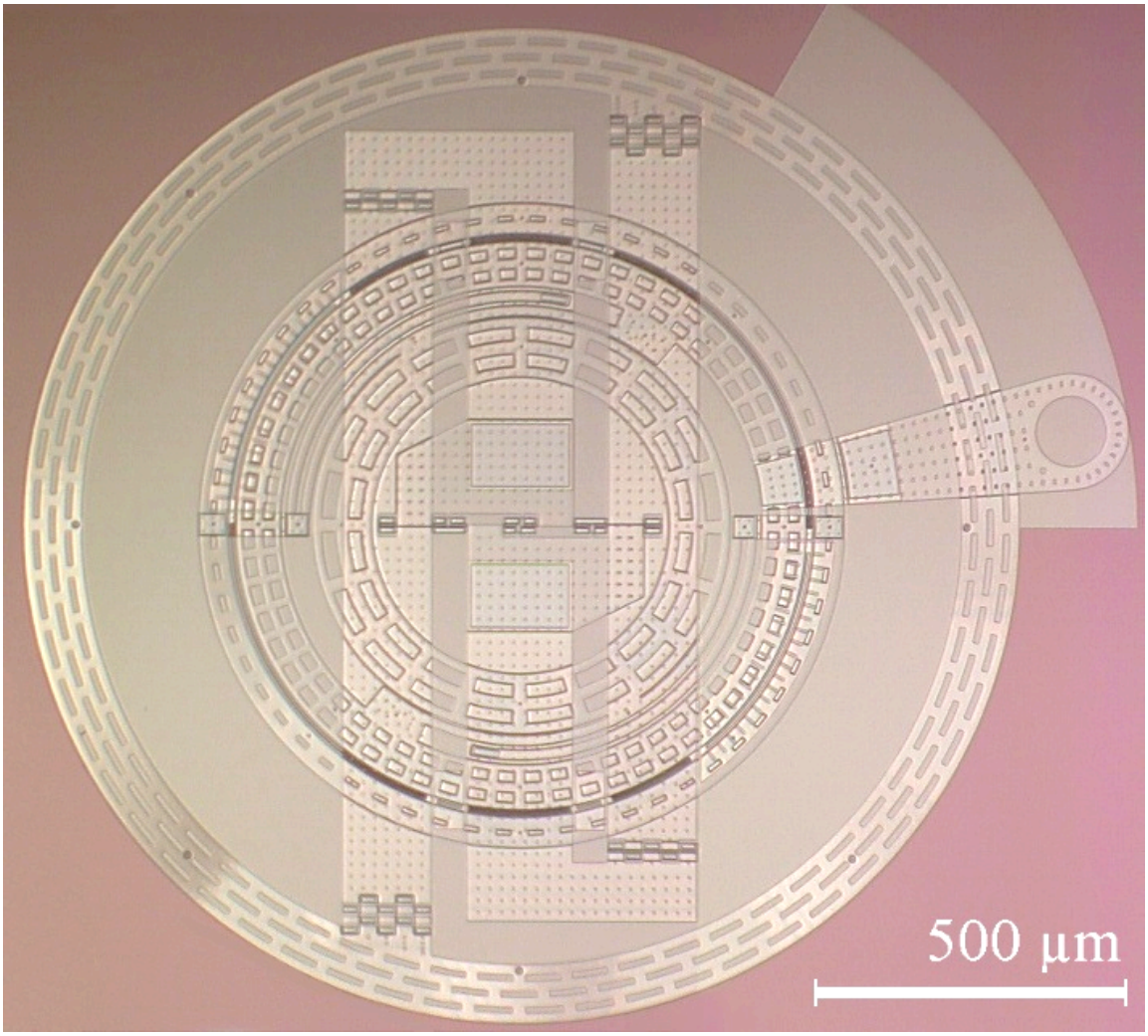

Figure 4.5 BAP seen through optical microscope

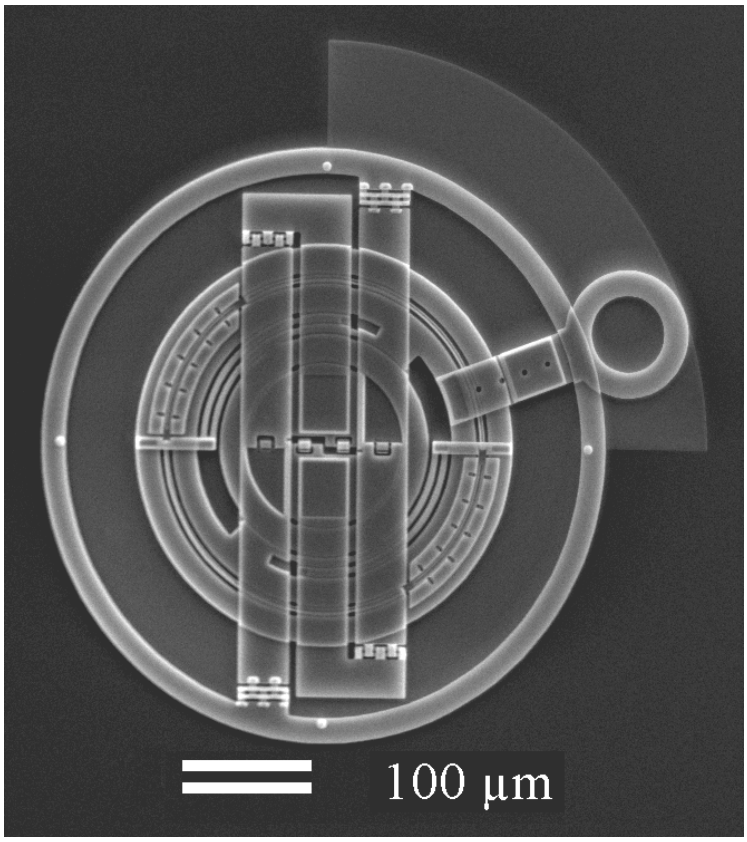

Figure 4.6 Small BAP seen through SEM

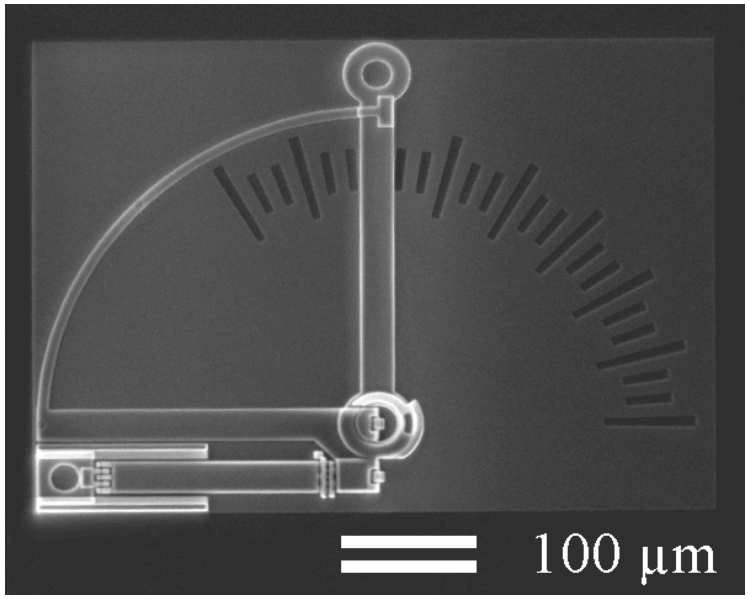

Figure 4.7 QBM seen through SEM

4.3. Testing Results

This version of the BAP mechanism was designed to be manually actuated through the use of probes, manipulators that allow the precise positioning of thin needles on the surface of a semiconductor device. A vacuum is utilized to secure the die against the movements of the probes. The probe tips are positioned above the die and are then touched down on the die surface; thus allowing the released MEMS to be manipulated by subtle movements of the probe, which can push, pull, and prod the mechanism.

Manipulating the mechanisms proved cumbersome, with the result being numerous broken devices. This is partly due to the fact that polysilicon shares many of the characteristics of glass and will tend to shatter. Fortunately, the effort was rewarded with a small measure of success. Shown below in Figure 4.8 is the larger variety BAP with a partially raised main platform. Unfortunately, further actuation of the mechanism

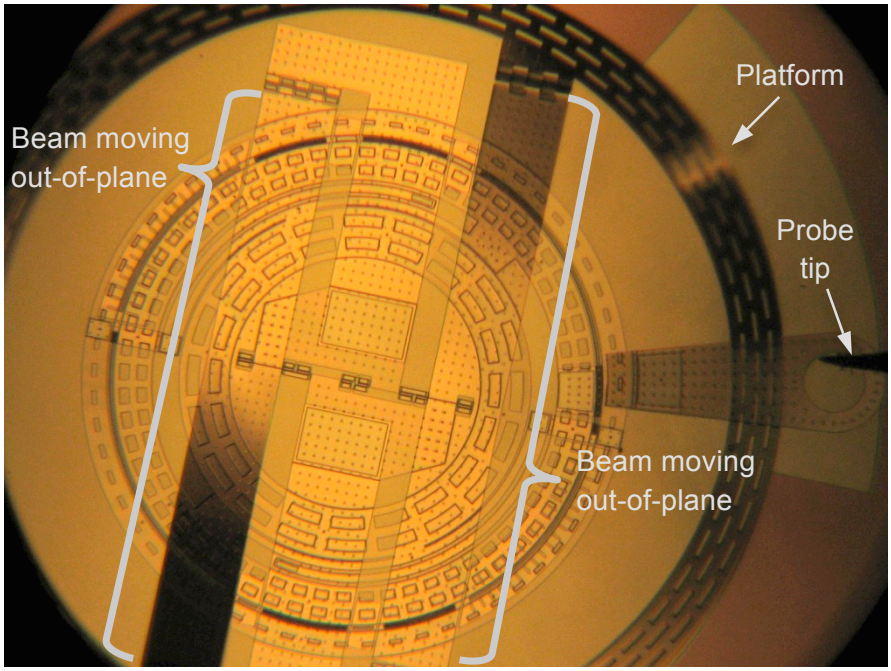

Figure 4.8 Partly actuated BAP with partially raised platform. Note the gradational shading on the out-of-plane beams and that the platform has moved out of focus.

immediately resulted in the fracture of the mechanism's handle. Figure 4.9 shows the small BAP following actuation.

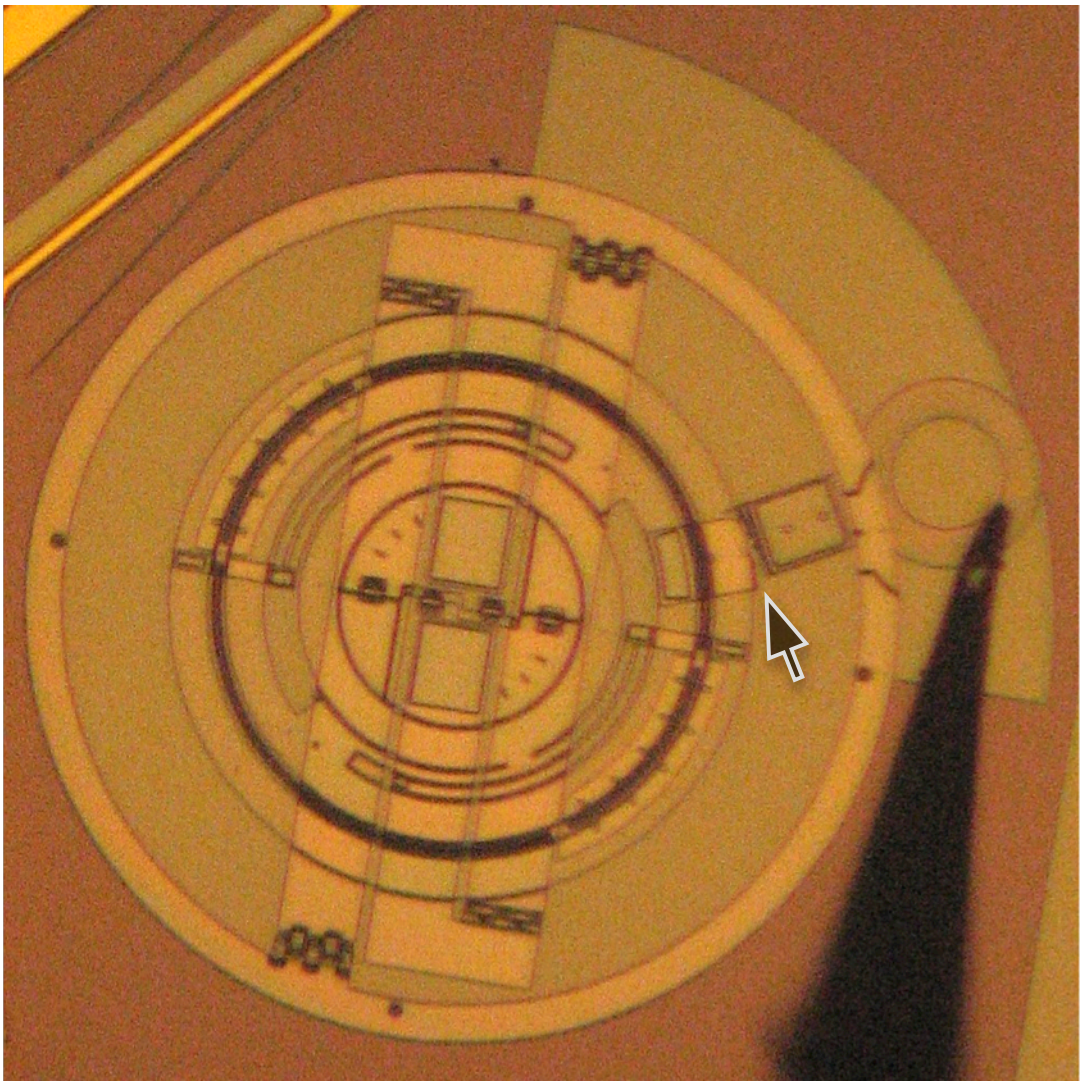

Figure 4.9 Small BAP with broken handle. The arrow indicates the point of fracture.

In both cases, the handle sheared off at its thinnest section where it passes over the guide ring for the planar links. Additional probing of the broken mechanism indicates that stiction was not interfering with its operation. In all probability, the fracture came about due to excessive friction and a concentration of stresses where the polysilicon

layers overlapped. The dimples used to eliminate stiction also served to reduce sliding friction along the substrate (underlying surface). However, when using the handle to rotate the ring that services the legs of the HKP, the edge of the ring is pressed up against its guides on the side opposite of the handle. The resulting imbalanced distribution of frictional forces is believed to have eventually caused the ring to bind and the handle to then shear off. In future iterations, manually actuated micro BAPs should include a second handle directly opposite of the first one in order to offset the frictional imbalance, which causes binding. A better alternative would be to incorporate rotary thermal actuators, which would evenly distribute the forces, keep the ring centered to avoid friction along the edges, and remove the human factor.

CHAPTER 5: QBM FORCE RELATIONSHIPS

The Quadrantal Bistable Mechanism is the crucial component of the Bistable Aerial Platform. The basic concept for the BAP design evolved from an observed force relationship in the QBM. Physical testing of a QBM model shows that an increase in the initial angle of the ortho-planar link yields a decrease in the requisite planar threshold force. Therefore, in order to quantify this relation, a simplified ANSYS model was developed.

5.1. Restrained ANSYS Model

The simplified model (whose ANSYS code is given in Appendix A) consists of only the quadrantal beam of the QBM, which is the only point of interest for observing the force relationship between the initial bias angle of the ortho-planar link and the planar threshold force required to actuate the QBM. Within the model, the ortho-planar end of the quadrantal beam was first displaced by a rotation θ, the angle of the ortho-planar link relative to its initial position. During the rotation of the ortho-planar end, the position of the planar end was held constant. Following this ortho-planar displacement, the ortho-planar end's new position was held constant while the planar end was displaced by a rotation of the planar link ϕ that increased from zero to five degrees of rotation in half degree increments, which was sufficient to ensure that the planar threshold force had been met for all cases. Once the planar end completed its motion, the beam reset to its initial position and the subsequent case began with a new θ, which increased incrementally by five degrees from zero to ninety (See flow chart in Figure 5.1).

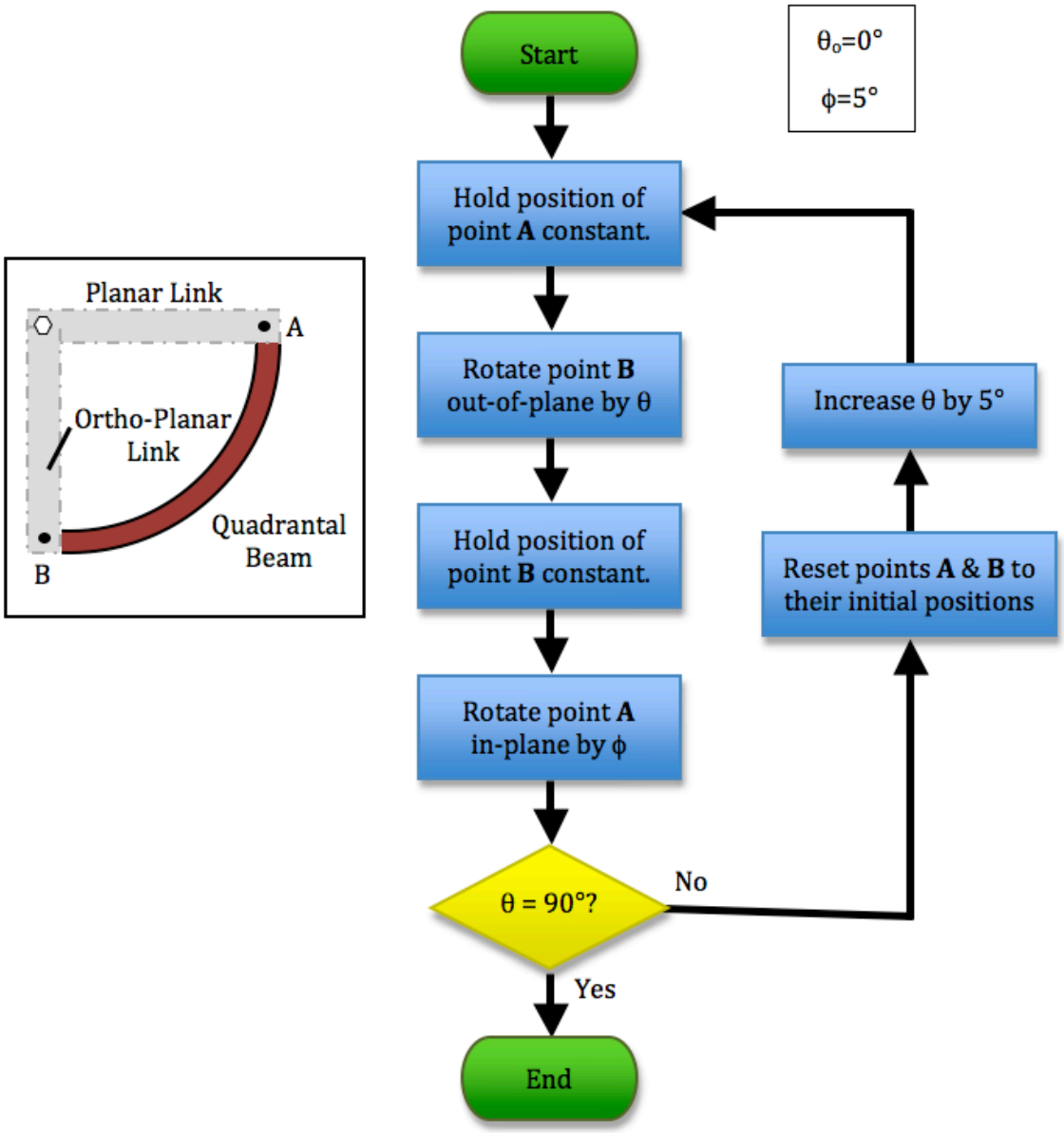

Figure 5.1 Flowchart of the restrained ANSYS model

The model was setup in this fashion in order to find the force applied to the QBM's planar link that will result in a reversal of the direction of the force on the ortho-planar link. At this instant, the planar threshold force needed for actuation has been met and the QBM will tend towards its second stable position. The initial angle of the ortho-planar link was varied so that the relationship between θ and the planar threshold force

could be observed. This is important because the BAP design requires an inverse relationship in order for the HKP to function as an actuator. Displacement loads were used in this model to insure that sufficient force had been applied to the planar links, since the planar threshold forces for the various bias angles were unknown prior to this analysis.

5.2. Coordinate Transformation

The ANSYS data provides the forces experienced by the model in terms of the original xyz coordinate system. However, in order to properly monitor the direction of the forces at the ends of the rotating links, the data taken from ANSYS must be transformed from the original frame of reference, O, into new frames, A and B, that rotate with the planar and ortho-planar links, respectively. The method used to accomplish the transformation is further explained in Appendix F.

The original and moving frames are shown below in Figure 5.2,

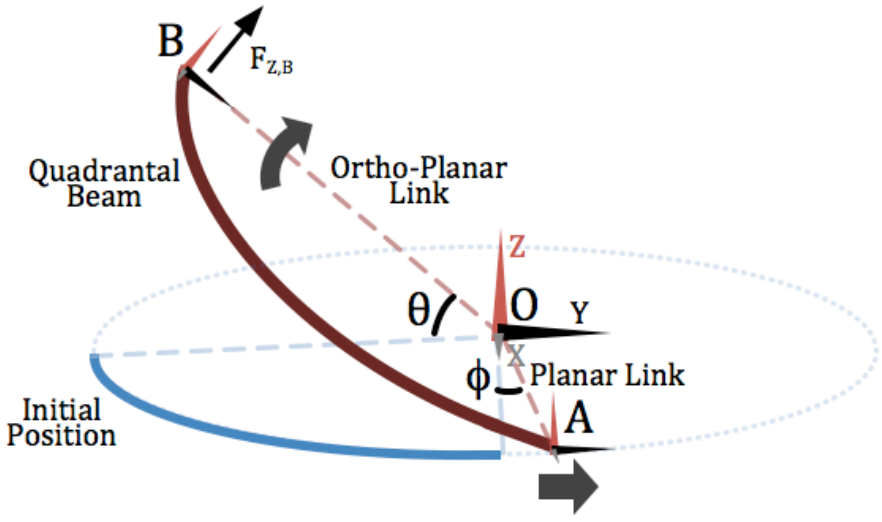

Figure 5.2 Rotating frames on the quadrantal beam

and will be transformed by

$$\vec{A} = R(O_z, \phi)\vec{O}. \tag{5.1}$$

$$\vec{B} = R(O_x, \theta)\vec{O}. \tag{5.2}$$

This means that the A-frame for the planar link represents a rotation of the O-frame about the original z-axis by ϕ, and that the B-frame represents a rotation about the x-axis by θ. Therefore,

$$[R_A] = \begin{bmatrix} \cos\phi & \sin\phi & 0 \\ -\sin\phi & \cos\phi & 0 \\ 0 & 0 & 1 \end{bmatrix} \tag{5.3}$$

and

$$[R_B] = \begin{bmatrix} 1 & 0 & 0 \\ 0 & \cos\theta & \sin\theta \\ 0 & -\sin\theta & \cos\theta \end{bmatrix}. \tag{5.4}$$

These rotation matrices will allow the force data provided by ANSYS to be adjusted for the planar and orth-planar links, thus allowing F_x, F_y, and F_z to be seen in terms of the relative position and orientation of the link.

5.3. Force Analysis

The observed decrease in the planar threshold force with an increased rotation of the ortho-planar link by θ, is fundamental to the operation of the BAP. To mathematically confirm this observation, the ANSYS data for the restrained model has been analyzed using MATLAB. In this analysis (See Appendix C for MATLAB code), the forces at the

ends of the planar and ortho-planar links have been transformed into their relative frames using the rotation matrices in equations (5.3) and (5.4).

The forces on the ortho-planar link are of particular concern in confirming the QBM force relationship. When the reaction force normal to the ortho-planar link, $F_{z,B}$ (F_z in the B-frame), changes from downward to upward, that is an indication that the planar threshold force on the planar link has been met and that the ortho-planar link will be pulled upward by the continued movement of the planar link. The MATLAB code was therefore programmed to find the value of the planar force (the planar threshold force) at which the $F_{z,B}$ changes sign. This was done for ortho-planar link rotations of $0 \leq \theta \leq 90^{\circ}$ in order to represent a wide range of initial biases applied to the ortho-planar link. The results of this analysis are illustrated by the graph in Figure 5.3, which confirms the QBM force relationship required for the BAP to function.

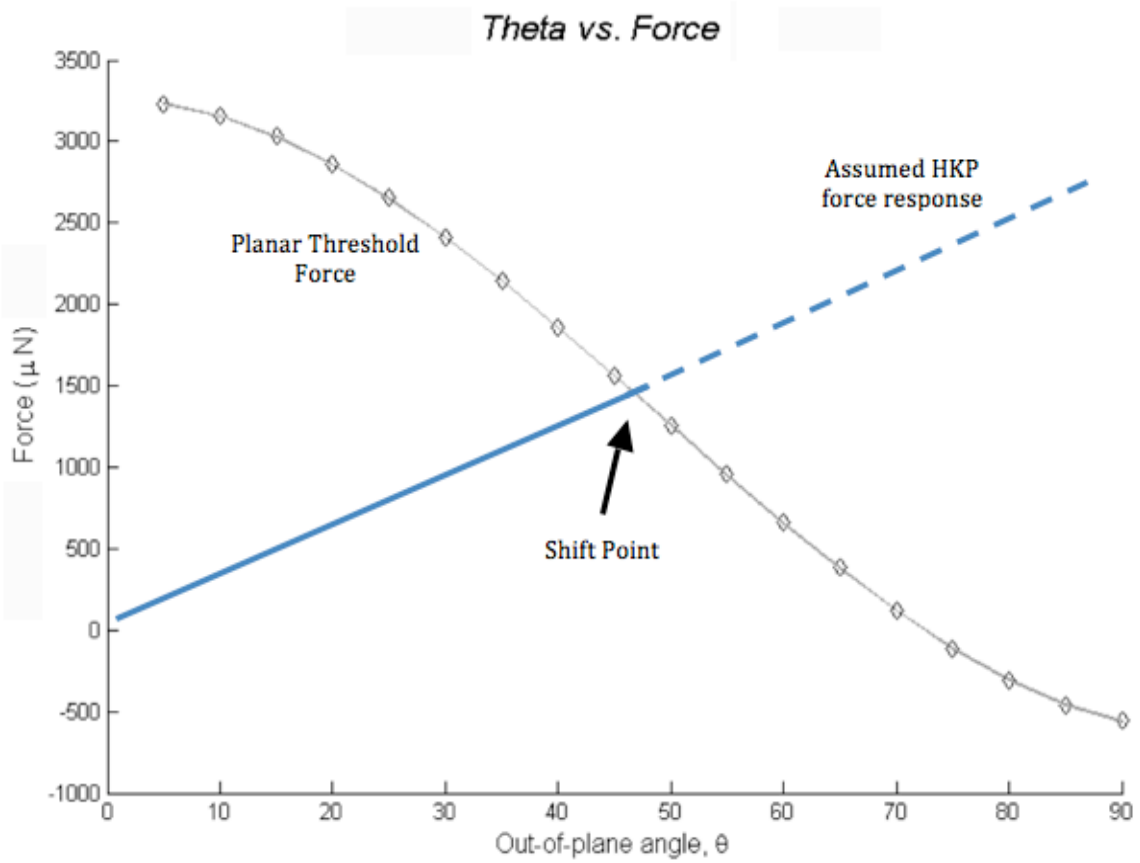

Figure 5.3 Planar threshold force & HKP force response vs. θ

Also shown in Figure 5.3 is an assumed force response of a HKP leg, within the BAP, raised by the same θ as shown in Figure 5.4. Another researcher is currently developing the PRBM of the HKP that will predict its actual force response, but for now, however, it is safe to assume that the force required to compress the HKP will increase with θ. At some point, the force curves will intersect when the force required to further compress the HKP leg is equal to the decreasing planar threshold force of the QBM. At this *shift point* (the unstable position as described in section 2.4), the forces on the ortho-planar links will tend to snap towards their second stable state, drawing the BAP's platform into the "up" position.

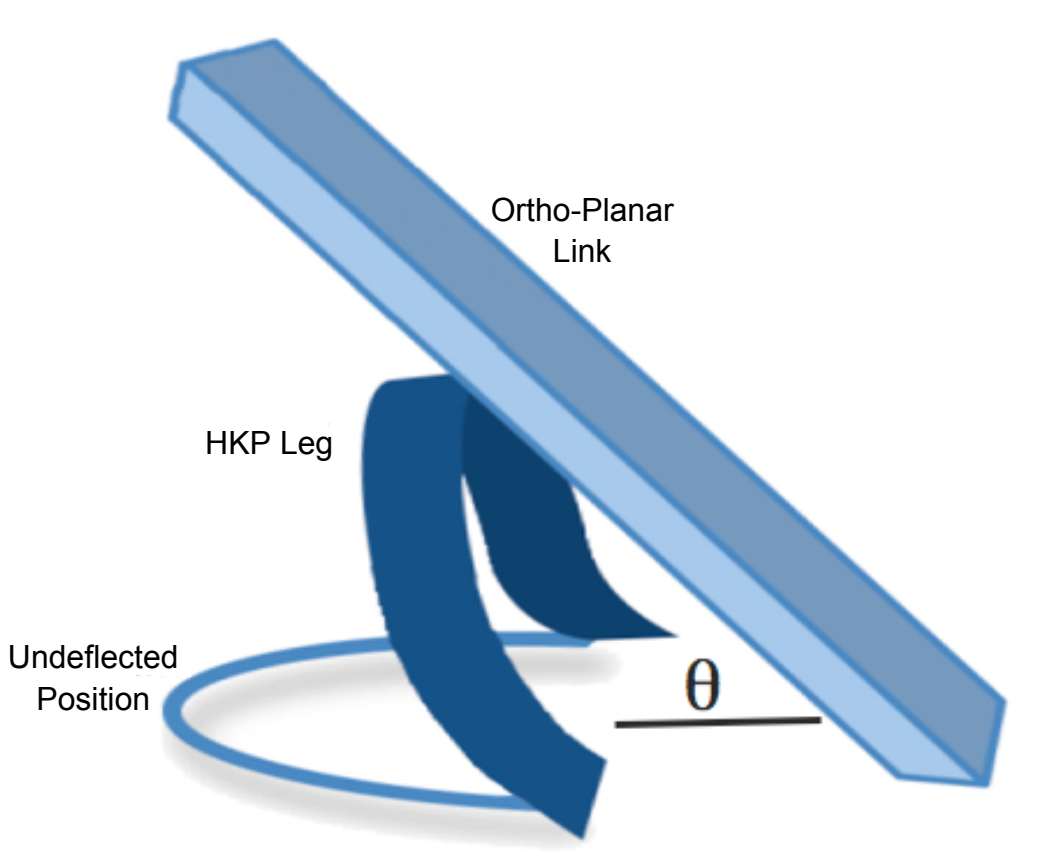

Figure 5.4 Ortho-planar link & HKP leg raised by θ

5.4. FEA of the Bistable Aerial Platform

A finite element analysis was also done on the Bistable Aerial Platform in order to confirm its general functionality (See Appendix E). The model used in this analysis (See Figure E.1) consisted of only the compliant components, the QBMs and the HKP. Contact elements were also included in order to permit the ortho-planar links to be raised by the elevating ring in the manner previously described.

As a displacement load compressed the legs of the HKP, the elevating ring rose as expected and lifted the ortho-planar links. However, in this model, which was based on the dimensions of the larger MEMS BAP, the planar force applied by the compressed

HKP legs never equaled the planar threshold force. Thus, it never achieved its second stable state.

However, applying an additional displacement load directly to the planar links, following the partial actuation achieved with just the elevating ring, provided that requisite planar threshold force and allowed the BAP to snap into its second stable state. This validates the basic concepts behind the design, but indicates that the QBMs and the HKP must be modified in order to properly balance the operant forces. Thus, a pseudo-rigid body model is needed in order to better understand these compliant mechanisms.

CHAPTER 6: QBM PSEUDO-RIGID BODY MODEL

Pseudo-rigid-body models (PRBMs) are developed by observing the deflection path of a compliant mechanism and then determining an equivalent rigid-body model that will follow the same approximate path. The chosen PRBM is then optimized until the error in the forces and deflection path between the compliant mechanism and its PRBM are minimized. In complex mechanisms, multiple models may be required before the error is brought to within acceptable tolerances. Therefore, in an effort to accelerate the development of a PRBM for the QBM, a model that has already been developed for a similar mechanism [5] will be modified to match the QBM, thus reducing some of the initial design work.

6.1. Related PRBM

The related PRBM that will be used to form the new PRBM of the QBM was done for a similar spherical mechanism that consists of the same planar and ortho-planar links with their corresponding axes, as well as an arc connecting the two links. This particular model was designed as a compliant spherical slider (See Figure 6.1) and addressed differing arc lengths and aspect ratios [5]. It is a simplified case that assumes that the arc does not sag inward due to tensile forces during manipulation of the adjoining links. This is achieved by imposing an unrealistic constraint on the center of the arc that maintains it at a constant radial distance from the origin by means of an applied force. This prior model also differs from the QBM as the arc is pinned to the ortho-planar link and not simply a single piece (See Figure 6.2 for PRBM).

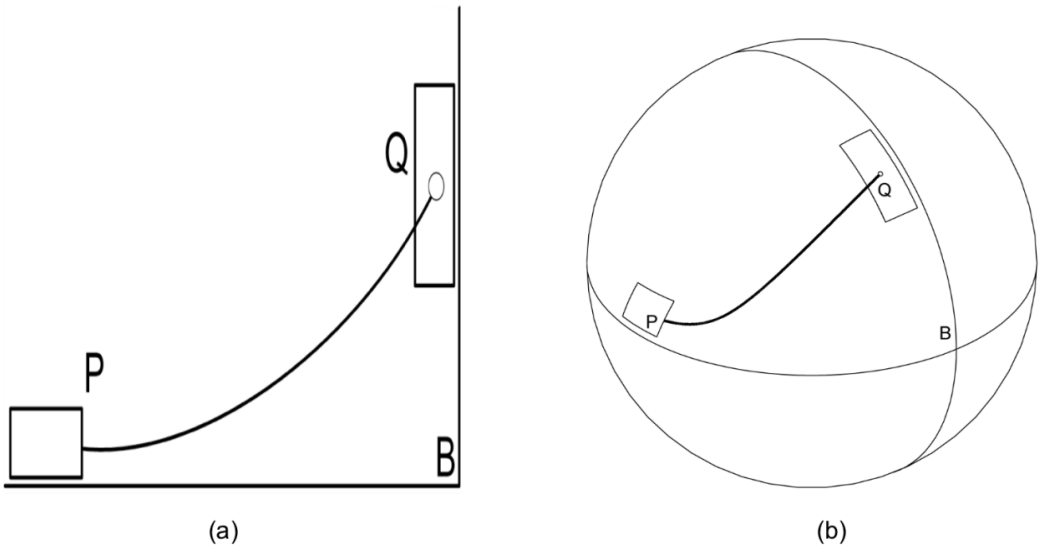

Figure 6.1 **(a)** Compliant planar slider with straight slides
(b) Compliant spherical slider with circular slides
[5] [4]

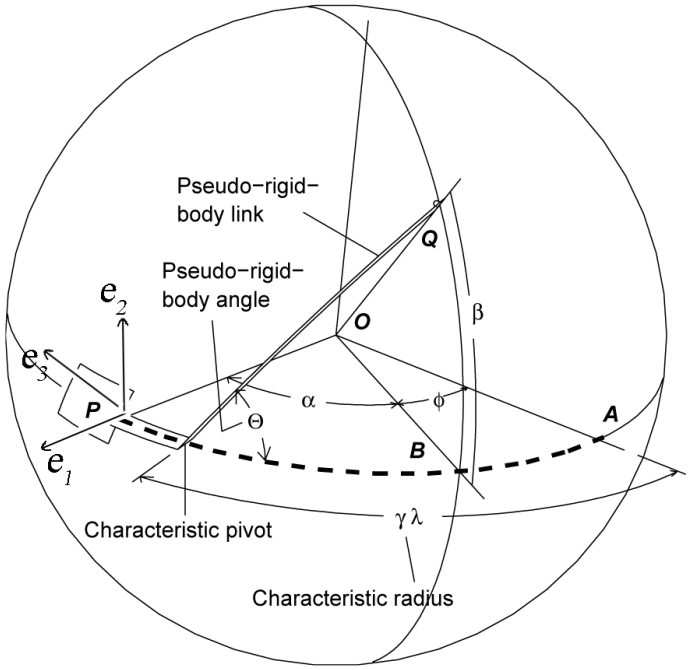

Figure 6.2 PRBM for a compliant spherical slider
[5] [5]

[4] Image used with permission.
[5] Image used with permission.

6.2. Preliminary PRBM of a Spherical Fixed-Guided Beam

The result of pinning the deflected end in the fixed-pinned PRBM model for the compliant spherical slider is the elimination of moments at the tip, which essentially causes it to behave as a free end with an applied force. Thus, the model developed by León [20] is in actuality a spherical fixed-free cantilever, similar to the planar fixed-free cantilever discussed in section 2.3.1. Furthermore, the QBM is essentially a spherical version of the fixed-guided beam, also discussed in section 2.3.2, which implies that a similar relationship will exist between the compliant spherical slider and the QBM as does between the planar fixed-free and fixed-guided beams. Therefore, the PRBM for the compliant spherical slider shown in Figure 6.2 will be used as a half model of the QBM to form the full model shown in Figure 6.4. This half model, with an arc length of forty-five degrees, will predict the deflected position of the quadrantal beam's center (See Figure 6.3).

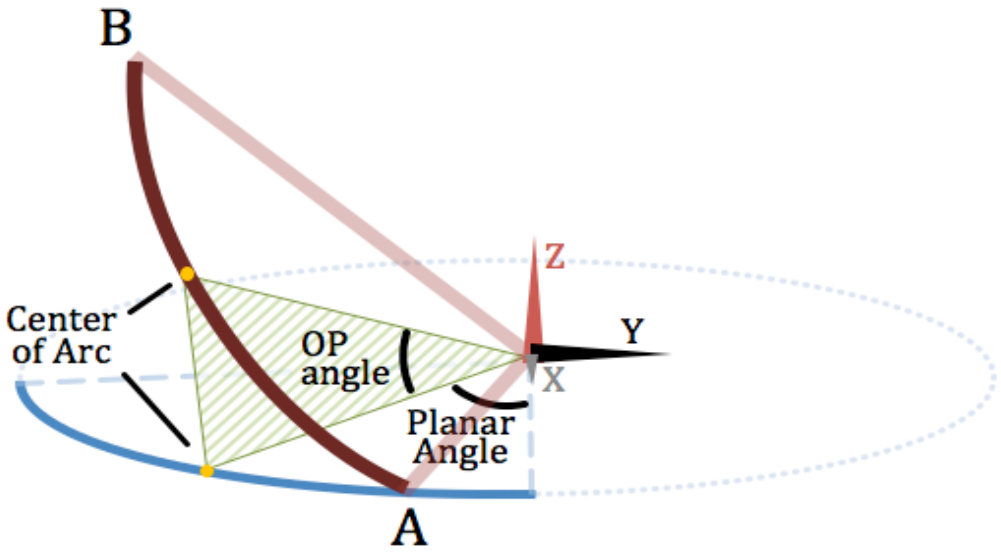

Figure 6.3 Angles measured by the half model for the QBM

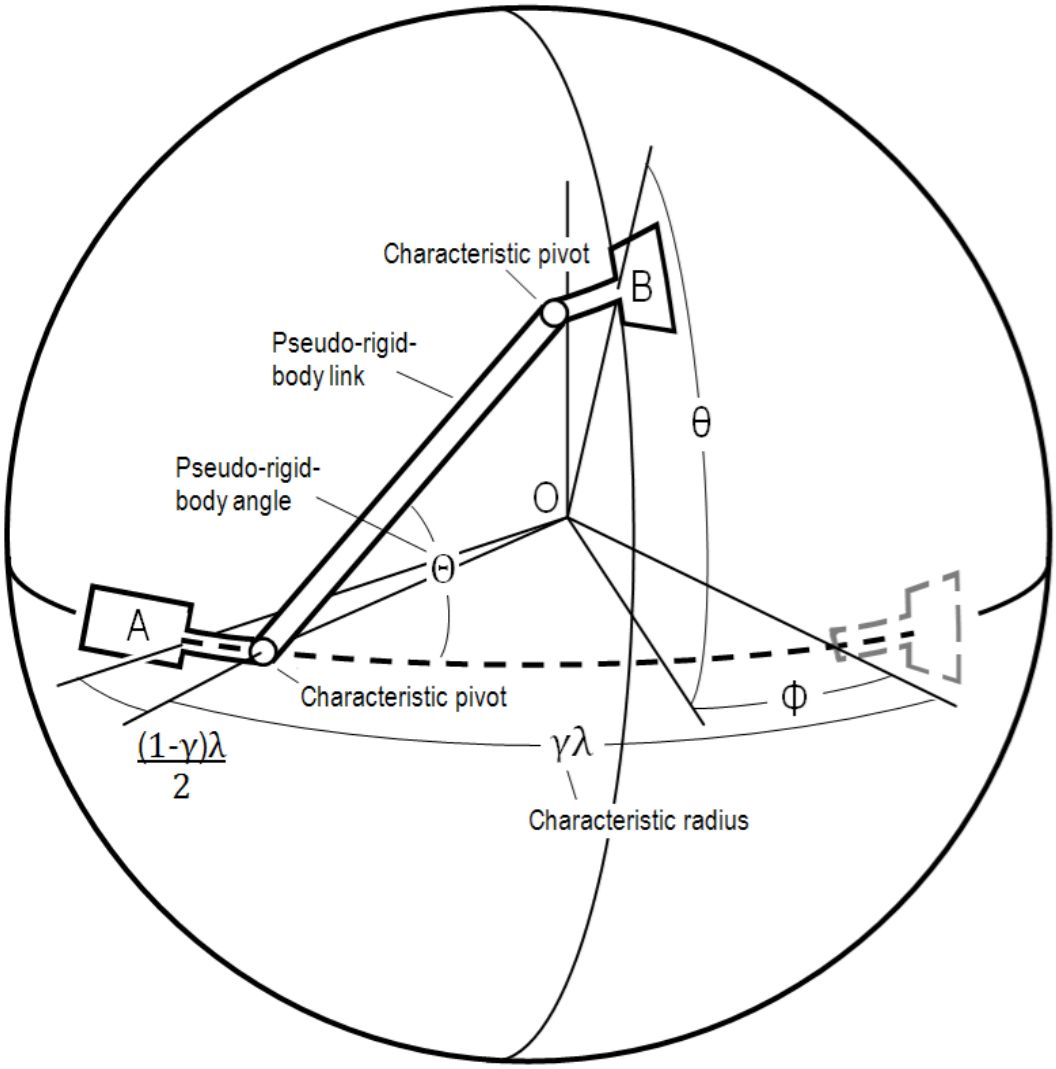

Figure 6.4 Full PRBM of the QBM

6.2.1. Unrestrained ANSYS Model

The intention of this ANSYS model for the QBM (See Appendix B) was to compare only the QBM's bending response to that of the preliminary PRBM of a spherical fixed-free cantilever, which currently does not address any type of elongation. Therefore, no displacement constraints were applied to the planar link so that the unrestrained planar link would be free to rotate to its minimum energy position. The model consists of the quadrantal beam and the planar link which limits one end of the

quadrantal beam to in-plane rotation about the z-axis. The ortho-planar end of the quadrantal beam is then raised out-of-plane by an angle θ which varies from 0 – 90˚.

6.2.2. Adequacy of the PRBM

The position analysis of the ANSYS data for the small BAP and the proposed PRBM for a spherical fixed-guided beam (See Appendix D for MATLAB code) was done with the results shown below. In Figure 6.5, the ortho-planar angle, relative to the origin, of the quadrantal beam's center, is shown. Note that the last two sets of data perfectly overlap, which would be an ideal case where the spherical quadrantal beam behaves the same as its planar cousin. The first set representing actual position data taken from the FEA, however, indicates that a significant amount of sag is occurring due to tensile forces. These tensile forces, which act along the quadrantal beam, cause it to flatten out its arc in order to accommodate the increased distance between the planar and ortho-planar links, thus sagging inward. In Figure 6.6, this inward drift of the center point becomes more apparent for the planar angle.

In spite of the problems caused by tensile forces which cause sagging, the deflections anticipated by the new, preliminary PRBM appear reasonable, especially since the points of interest will typically be the rigid links which will not deform. The forces and moments anticipated by the PRBM, however, do not appear reasonable as is shown in Figure 6.7. This is caused not only by the deformation of the quadrantal beam due to tensile forces, which the prior PRBM neglected, but also by the prior PRBM's imposed constraint on the arc itself that maintained it at a constant radius. Therefore, the values of the torsional spring constants must be adjusted to reflect these oversights.

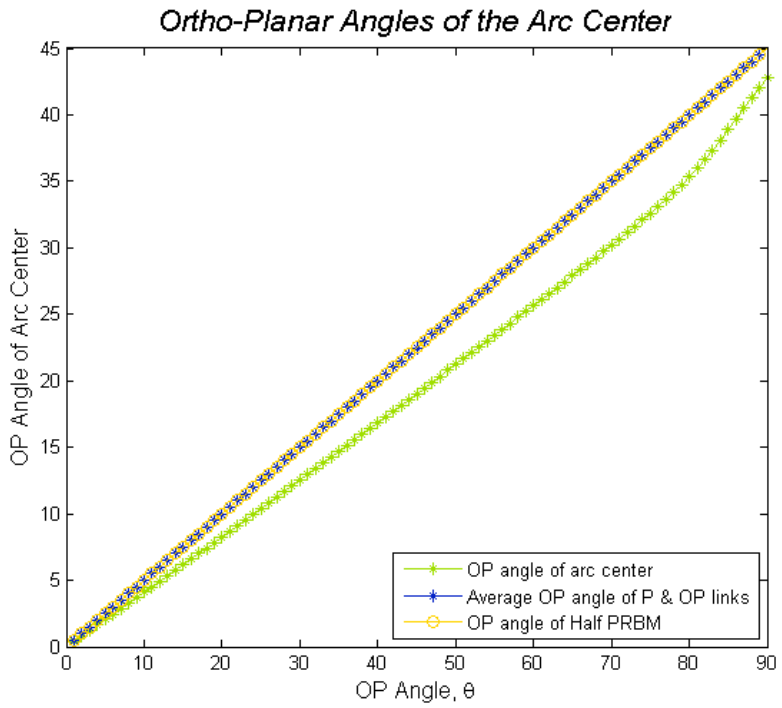

Figure 6.5 Ortho-planar angle of the quadrantal beam's center vs. θ

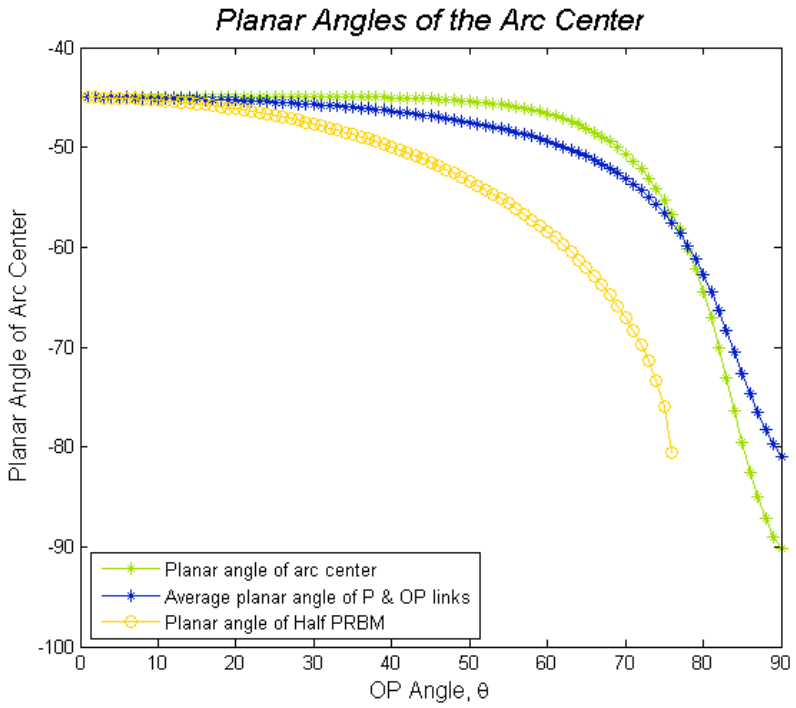

Figure 6.6 Planar angle of the quadrantal beam's center vs. θ

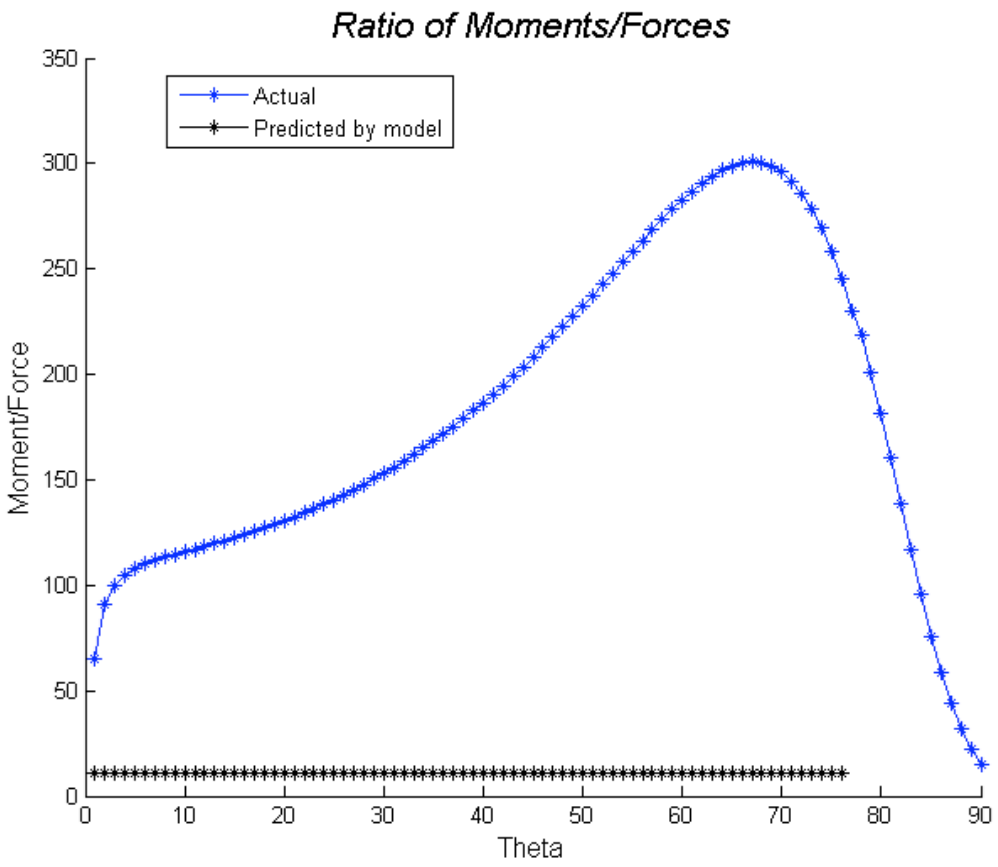

Figure 6.7 Ratio of the moments to forces in the PRBM and the actual QBM

6.2.3. Possible PRBM Improvements

Modifications to the PRBM must be made in order to more accurately model the elongating quadrantal beam of the QBM. One possible alteration is to have the overall length of the model increase as θ increases. A quick attempt at this was tried with the results shown in Figure 6.8. As indicated by the graph, linearly increasing the arc length, λ, with increasing θ causes the planar angle to more closely match the actual planar angle of the compliant quadrantal beam. However, the relation is most likely non-linear, and further research will be required to discover the proper relationship.

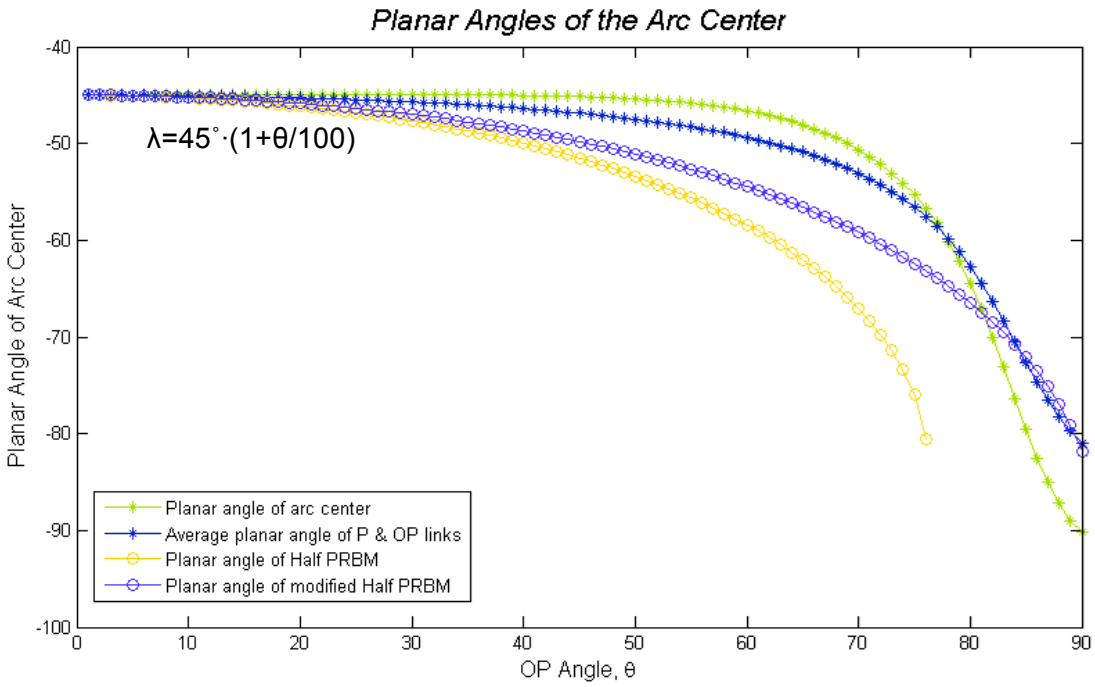

Figure 6.8 Planar angle vs. θ with linearly increasing arc length

Another possible way of accounting for the increasing arc length would be through the addition of another spring at the center of the arc to allow the beam to stretch. This spring approach, while more complex, may prove the better method because it can also address the condition when a force is applied on the planar link of the QBM, such as in the BAP. Accurately modeling the forces and moments is probably even more important than capturing the position of the beam. Therefore, adjusting the spring constants for the torsional springs and this additional spring, meant to capture the energy stored by the elongation of the quadrantal beam, should be the primary focus in completing the PRBM.

CHAPTER 7: RESULTS AND DISCUSSION

7.1. BAP Design

While the current iteration of the BAP will require additional refinement to reach its second state, the principle behind the design remains valid. The QBM force relationship, the fundamental theory on which the QBM is based, has been proven. Additionally, both the MEMS prototype and the finite element analysis of the BAP itself (See Appendix E) show the desired upward movement of the platform as the HKP lifts the ortho-planar links. Unfortunately, the handle breaks during actuation of the prototype and the FEA model shows that the forces applied by the HKP legs on the planar links are insufficient to provide the necessary planar threshold force.

Once the HKP and QBM forces are balanced, the BAP should move smoothly into its second state. However, because the compliant mechanisms involved are not yet fully understood and their PRBMs are not yet fully developed, properly balancing the forces to improve the mechanism can only be achieved through the trial and error of adjusting the arc length, aspect ratio, radius, etc. In the meantime, an additional rotational displacement load can be applied directly to the planar links, once the BAP is partially actuated, to provide the necessary planar threshold force. The ANSYS model for the large MEMS BAP prototype currently indicates that a small rotary displacement of the planar link is all that is required to get the mechanism to its “up” stable position. This implies that only a few subtle changes to the BAP are required to achieve the desired result unaided. The FEA model of the BAP therefore further proves the validity of the

overall design and also serves as a justification for further research into compliant mechanisms.

7.2. QBM PRBM

Great progress has been made toward the development of a PRBM for the QBM. A preliminary PRBM of a spherical fixed-guided beam has been developed that, in its current state, reasonably models the positional bending response of the QBM. However, further development is needed to capture the force and moment response and to model the elongation of the quadrantal beam due to tensile forces. Once the PRBM is perfected, it will serve to balance the forces within the BAP by adjusting various physical aspects of the QBM and will work in conjunction with the PRBM of the HKP, which is also currently under development.

REFERENCES

[1] Ananthasuresh, G. K., Sridhar Kota, and Yogesh Gianchandani. "Systematic Synthesis of Microcompliant Mechanisms - Preliminary Results." University of Michigan, 1993.

[2] Fujita, Hiroyuki. "A Decade of MEMS and its Future." Institute of Industrial Science, The University of Tokyo, 1997.

[3] Howell, Larry L. "A Generalized Loop-Closure Theory for the Analysis and Synthesis of Compliant Mechanisms." PhD Thesis, Purdue University, West Lafayette, 1993.

[4] Lusk, Craig P. "Ortho-Planar Mechanisms for Microelectromechanical Systems." PhD Thesis, Brigham Young University, Provo, 2005.

[5] León, Alejandro, Saurabh Jagirdar, and Craig P. Lusk. "A Pseudo-Rigid-Body Model for Spherical Mechanisms: The Kinematics of a Compliant Curved Beam." *Proceedings of IDETC/CIE.* New York: ASME, 2008.

[6] Frazier, Bruno, Robert O. Warrington, and Craig Friedrich. "The Miniaturization Technologies: Past, Present, and Future." *IEEE Transactions on Industrial Electronics* 42, no. 5 (1995): 423-430.

[7] Gabriel, Kaigham J. "Microelectromechanical Systems (MEMS) Tutorial." (Carnegie Mellon University) 1998.

[8] Koester, David A., Karen W. Markus, and Mark D. Walters. "MEMS: Small machines for the microelectronics age." (MCNC MEMS Technology Applications Center) January 1996: 93-94.

[9] Ananthasuresh, G. K., and Sridhar Kota. "Designing Compliant Mechanisms." *Mechanical Engineering*, Nov. 1995: 93-96.

[10] Howell, L. L., A. Midha, and T. W. Norton. "Evaluation of Equivalent Spring Stiffness for Use in a Pseudo-Rigid-Body Model of Large-Deflection Compliant Mechanisms." *Journal of Mechanical Design* 118 (March 1996): 126-131.

[11] Canfield, S. L., J. W. Beard, N. Lobontiu, E. O'Malley, M. Samuelson, and J. Paine. "Development of a Spatial Compliant Manipulator." *International Journal of Robotics and Automation* 17, no. 1 (2002): 63-70.

[12] Frecker, Mary, and Noboru Kikuchi. "Optimal Synthesis of Compliant Mechanisms to Satisfy Kinematic and Structural Requirements - Preliminary Results." *Computers in Engineering Conference.* Irvine: ASME, 1996. 1-9.

[13] Kota, S., G. K. Ananthasuresh, S. B. Crary, and K. D. Wise. "Design and Fabrication of Microelectromechanical Systems." *Journal of Mechanical Design* 116 (December 1994): 1081-1088.

[14] Howell, L. L., and A. Midha. "A Method for the Design of Compliant Mechanisms With Small-Length Flexural Pivots." *Transactions of the ASME* 116 (March 1994): 280-290.

[15] Howell, Larry. *Compliant Mechanisms.* New York: John Wiley & Sons, Inc., 2001.

[16] Foulds, I., M. Trinh, S. Hu, S. Liao, R. Johnstone, and M. Parameswaran. "A Surface Micromachined Bistable Switch." *Proceedings of the 2002 IEEE Canadian Conference on Electrical & Computer Engineering.* IEEE, 2002. 465-469.

[17] Opdahl, Patrick G., Brian D. Jensen, and Larry L. Howell. "An Investigation Into Compliant Bistable Mechanisms." *Design Engineering Technical Conferences.* Atlanta: ASME, 1998. 1-10.

[18] Chiang, C. H. "Spherical Kinematics in Contrast to Planar Kinematics." *Mechanism and Machine Theory* 27, no. 3 (1992): 243-250.

[19] Jagirdar, Saurabh. "Kinematics of Curved Flexible Beam." M.S. Thesis, University of South Florida, Tampa, 2006.

[20] León, Alejandro. "A Pseudo-Rigid-Body Model For Spherical Mechanisms: The Kinematics and Elasticity of a Curved Compliant Beam." M.S. Thesis, University of South Florida, Tampa, 2007.

[21] Koester, David, Allen Cowen, Ramaswamy Mahadevan, Mark Stonefield, and Busbee Hardy. *PolyMUMPs Design Handbook.* 10. MEMSCAP, 2003.

[22] Kolpekwar, Abhijeet, R. D. Blanton, and David Woodilla. "Failure Modes for Stiction in Surface-Micromachined MEMS." *International Test Conference.* IEEE, 1998. 551-556.

[23] Muller, Richard S. "MEMS: Quo Vadis in Century XXI." *Microelectronic Engineering* (Elsevier) 53 (2000): 47-54.

[24] Alley, R. L., G. J. Cuan, R. T. Howe, and K. Komvopoulos. "The Effect of Release-Etch Processing on Surface Microstructure Stiction." Department of Electrical Engineering and Computer Sciences, University of California at Berkeley, 1992.

[25] Bhushan, Bharat. *Nanotribology and Nanomechanics of MEMS Devices.* Department of Mechanical Engineering, The Ohio State University, Columbus: IEEE, 1996, 91-98.

[26] Hestenes, David. *New Foundations for Classical Mechanics.* Edited by Alwyn Van Der Merwe. Dordrecht: D. Reidel Publishing Company, 1986.

APPENDICES

Appendix A: ANSYS Code for a Restrained QBM

```
!*****************************************
!/INPUT,J:\Thesis\ANSYS\QBM_restrained,txt,,1
!/CWD,'J:\Thesis\ANSYS'
!*****************************************

FINISH
/CLEAR

/FILENAME, Restrained Quadrantal Bistable Mechanism
/title,Restrained Quadrantal Bistable Mechanism


WRITE=1                          ! 1= Write output files,
                                 ! Else= Don't Write

/PREP7                           ! Enter the pre-processor

!*****************************************
!********** Model Parameters *************
!*****************************************

OP_Start=0                       ! Theta for first case
(multiple of 5)
OP_Stop=90                       ! Theta for final case
(multiple of 5)

PI=acos(-1.)

R=100                            ! Radius of quadrantal beam
h=2                              ! Thickness
b=5                              ! Width of compliant segments

!************ Define Area ****************

A = h*b                         ! Cross sectional area of beams
Iz= 1/12*b*h*h*h                ! Second Moment of Area
                                ! (aka Area Moment of Inertia)
Ix= 1/12*h*b*b*b

!*****************************************
!********** Define Keypoints *************
!*****************************************

! Create Keypoints: K(Point #, X-Coord, Y-Coord, Z-Coord)

K,1,0,0,0,
K,2,0,-R,0,
K,3,R,0,0,
```

Appendix A (Continued)

```
!*****************************************
!************ Create Links ***************
!*****************************************

LARC,2,3,1,R,                   ! *Compliant*
LESIZE,ALL,,,32                 ! Divides the compliant arc
                                ! into 32 segments
!L,1,2,1

!******** Declare element type  **********
ET,1,BEAM4
KEYOPT,1,2,1
KEYOPT,1,6,1

!******** Define Real Constants **********
R,1,A,Ix,Iz,h,b,              ! Properties of compliant segments

!****** Define Material Properties ******
MP,EX,1,170000                ! Young's Modulus of Elasticity
                              ! (MPa)
MP,PRXY,1,0.22                ! Poisson's ratio

!*****************************************
!***************** Mesh ******************
!*****************************************

type,1                          ! Use element type 1
mat,1                           ! use material property set 1
real,1                          ! Use real constant set 1
LMESH,ALL                       ! mesh all lines

!******** Get Node # of keypoints ********

ksel,s,kp,,2
nslk,s
*get,nkp2,node,0,num,max        ! Retrieves and stores a value as a
                                ! scalar or part of an array

ksel,s,kp,,3
nslk,s
*get,nkp3,node,0,num,max

ALLSEL
FINISH                          ! Finish pre-processing

!*****************************************
!************* Solution ******************
!*****************************************

*get,date,active,,dbase,ldate
*get,time,active,,dbase,ltime

year=nint(date/10000)
month=nint(nint(date-year*10000)/100)
day=date-(nint(date/100))*100
```

Appendix A (Continued)

```
hour=nint(time/10000-.5)
minute=nint((time-hour*10000)/100-.5)

*DO,nn,OP_Start,OP_Stop,5

OPlanar_angle=nn                !Theta
Planar_angle =25                !Phi

KEYW,PR_SGUI,1                  ! Suppresses "Solution is Done"
                                ! text box
/SOL                            ! Enter the solution processor

/gst,off                        ! Turn off graphical convergence
monitor
ANTYPE,0                        ! Analysis type, static
NLGEOM,1                        ! Includes large-deflection effects
                                ! in a static or full transient
                                ! analysis
LNSRCH,AUTO                     ! ANSYS automatically switches line
                                ! search on/off
NEQIT,50                        ! Set max # of iterations
DELTIM,,0.0001                  ! Set minimum time step increment

!*****************************************
!**** Define Displacement Constraints*****
!*****************************************

DK,2,,0,,,UX,UY,UZ,ROTX,ROTY,ROTZ
DK,3,,0,,,UX,UY,UZ,ROTX,ROTY,ROTZ

!********* Displacement Load *************

LS1=OPlanar_angle

*IF,LS1,GT,0,THEN              ! "If" statement used to avoid the
                                ! warning when LS1=0 thus making
                                ! the "Do loop" unnecessary
*DO,step,1,LS1,1
theta=step*PI/180

disp2y=-R*cos(theta)+R
disp2z=R*sin(theta)

DK,2,UY,disp2y
DK,2,UZ,disp2z

LSWRITE,step
*ENDDO
*ENDIF

LS2=Planar_angle*2
*DO,step,1,LS2,1
phi=0.5*step*PI/180
```

Appendix A (Continued)

```
disp3x=R*cos(phi)-R
disp3y=R*sin(phi)

DK,3,UX,disp3x
DK,3,UY,disp3y

LSWRITE,LS1+step
*ENDDO

LS=LS1+LS2

LSSOLVE,1,LS

FINISH                          ! Finish the solution processor

!*****************************************
!*********** Postprocessor ***************
!*****************************************
/POST1                          ! Enter the postprocessor

PLDISP,1                        ! Displays deformed & undeformed
                                ! shape
/VIEW,1,1                       ! Switches to right view
/ANG,1,-90,ZS,0                 ! Rotates View
/ANG,1,15,XS,1                  ! Rotates View

SET,LAST
/REPLOT

*DIM,OPlanar,TABLE,LS,6
*DIM,Planar,TABLE,LS,6

*Do,i,1,LS
SET,i                           ! Read data for step "i"
*GET,fx1,Node,nkp2,RF,FX        ! Assign Ortho-planar data to
                                ! OPlanar table
*SET,OPlanar(i,1),fx1
*GET,fy1,Node,nkp2,RF,FY
*SET,OPlanar(i,2),fy1
*GET,fz1,Node,nkp2,RF,FZ
*SET,OPlanar(i,3),fz1
*GET,mx1,Node,nkp2,RF,MX
*SET,OPlanar(i,4),mx1
*GET,my1,Node,nkp2,RF,MY
*SET,OPlanar(i,5),my1
*GET,mz1,Node,nkp2,RF,MZ
*SET,OPlanar(i,6),mz1

*GET,fx1,Node,nkp3,RF,FX        ! Assign planar data to Planar
                                ! table
*SET,Planar(i,1),fx1
*GET,fy1,Node,nkp3,RF,FY
*SET,Planar(i,2),fy1
*GET,fz1,Node,nkp3,RF,FZ
*SET,Planar(i,3),fz1
```

Appendix A (Continued)

```
*GET,mx1,Node,nkp3,RF,MX
*SET,Planar(i,4),mx1
*GET,my1,Node,nkp3,RF,MY
*SET,Planar(i,5),my1
*GET,mz1,Node,nkp3,RF,MZ
*SET,Planar(i,6),mz1

*ENDDO

*IF,WRITE,EQ,1,THEN
*cfopen,J:\Thesis\ANSYS\Results\QBM_DATA_Theta=%OPlanar_angle%,te
xt

*vwrite,month,'-',day,'-',year,hour,':',minute
%I %C %I %C %I %4.2I %C %2.2I

*vwrite,'Note: The first',OPLanar_angle,'steps correspond to the
movement','of the Ortho-Planar link.','The final',LS2,'correspond
to the planar link.'
%C %I %C %C %/ %14C %I %C %/


*vwrite,'Planar:','angle phi = ',Planar_angle,'degrees'
%-17C %C %I %C

*vwrite,'FX','FY','FZ','MX','MY','MZ'
%-17C %-17C %-17C %-16C %-16C %-16C


*vwrite,Planar(1,1),Planar(1,2),Planar(1,3),Planar(1,4),Planar(1,
5),Planar(1,6)
%16.8G %16.8G %16.8G %16.8G %16.8G %16.8G


*vwrite,'Ortho-Planar:','angle theta = ',OPlanar_angle,'degrees'
%/ %/%-17C %C %I %C

*vwrite,'FX','FY','FZ','MX','MY','MZ'
%-17C %-17C %-17C %-16C %-16C %-16C


*vwrite,OPlanar(1,1),OPlanar(1,2),OPlanar(1,3),OPlanar(1,4),OPlan
ar(1,5),OPlanar(1,6)
%16.8G %16.8G %16.8G %16.8G %16.8G %16.8G

*cfclose
*ENDIF

FINISH
*ENDDO
```

Appendix A (Continued)

```
!*****************************************
/POST1                          ! Re-enter the postprocessor
                                ! following loops

PLDISP,1                        ! Displays deformed & undeformed
                                ! shape
/VIEW,1,1                       ! Switches to right view
/ANG,1,-90,ZS,0                 ! Rotates View
/ANG,1,15,XS,1                  ! Rotates View

SET,LAST
/REPLOT
/FOC,1,AUTO,,,1
/FOC,1,-0.5,-0.05,,1
/REPLOT

ANTIME,45,0.1, ,1,1,0,0         ! Animate
```

Appendix B: ANSYS Code for an Unrestrained QBM

```
!*****************************************
!/INPUT,J:\Thesis\ANSYS\QBM_unrestrained,txt,,1
!/CWD,'J:\Thesis\ANSYS'
!*****************************************

FINISH
/CLEAR

/FILENAME, Unrestrained Quadrantal Bistable Mechanism
/title, Unrestrained Quadrantal Bistable Mechanism


WRITE=1                          ! 1= Write output files,
                                 ! Else= Don't Write

/PREP7                           ! Enter the pre-processor

!*****************************************
!********** Model Parameters *************
!*****************************************

PI=acos(-1.)

R=100                            ! Radius of quadrantal beam
h=2                              ! Thickness
b=5                              ! Width of compliant segments

!************ Define Area ****************

A = h*b                         ! Cross sectional area of beams
Iz= 1/12*b*h*h*h                ! Second Moment of Area
                                 ! (aka Area Moment of Inertia)
Ix= 1/12*h*b*b*b

!*****************************************
!********** Define Keypoints *************
!*****************************************

! Create Keypoints: K(Point #, X-Coord, Y-Coord, Z-Coord)

K,1,0,0,0,
K,2,0,-R,0,
K,3,R,0,0,
K,4,R*cos(-45*PI/180),R*sin(-45*PI/180),0,
```

Appendix B (Continued)

```
!*****************************************
!************ Create Links ***************
!*****************************************

L,1,3,1
LARC,2,4,1,R,                  ! *Compliant*
LARC,4,3,1,R,                  ! *Compliant*
LESIZE,2,,,16                  ! Divides the compliant arc into 16
                               ! segments
LESIZE,3,,,16                  ! Divides the compliant arc into 16
                               ! segments

!******** Declare element type  **********
ET,1,BEAM4
KEYOPT,1,2,1
KEYOPT,1,6,1

!******** Define Real Constants **********
R,1,A,Ix,Iz,h,b,               ! Properties of compliant segments

!****** Define Material Properties ******
MP,EX,1,170000                 ! Young's Modulus of Elasticity
                               ! (MPa)
MP,PRXY,1,0.22                 ! Poisson's ratio

!*****************************************
!***************** Mesh ******************
!*****************************************

type,1                          ! Use element type 1
mat,1                           ! use material property set 1
real,1                          ! Use real constant set 1
LMESH,ALL                       ! mesh all lines

!******** Get Node # of keypoints ********

ksel,s,kp,,1
nslk,s
*get,nkp1,node,0,num,max       ! Retrieves and stores a value as a
                               ! scalar or part of an array

ksel,s,kp,,2
nslk,s
*get,nkp2,node,0,num,max

ksel,s,kp,,3
nslk,s
*get,nkp3,node,0,num,max
```

Appendix B (Continued)

```
ksel,s,kp,,4
nslk,s
*get,nkp4,node,0,num,max

ALLSEL
FINISH                          ! Finish pre-processing

!*****************************************
!************* Solution ******************
!*****************************************

*get,date,active,,dbase,ldate
*get,time,active,,dbase,ltime

year=nint(date/10000)
month=nint(nint(date-year*10000)/100)
day=date-(nint(date/100))*100
hour=nint(time/10000-.5)
minute=nint((time-hour*10000)/100-.5)


OPlanar_angle=90                !Theta

KEYW,PR_SGUI,1                  ! Suppresses "Solution is Done"
                                ! text box
/SOL                            ! Enter the solution processor

/gst,off                        ! Turn off graphical convergence
                                ! monitor
ANTYPE,0                        ! Analysis type, static
NLGEOM,1                        ! Includes large-deflection effects
                                ! in a static or full transient
                                ! analysis
LNSRCH,AUTO                     ! ANSYS automatically switches line
                                ! search on/off
NEQIT,50                        ! Set max # of iterations
DELTIM,,0.0001                  ! Set minimum time step increment

!*****************************************
!**** Define Displacement Constraints*****
!*****************************************

DK,1,,0,,,UX,UY,UZ,ROTX,ROTY
DK,3,,0,,,UZ
```

Appendix B (Continued)

```
!********* Displacement Load *************

*DO,step,1,OPlanar_angle,1
theta=step*PI/180

disp2y=-R*cos(theta)+R
disp2z=R*sin(theta)

DK,2,UY,disp2y
DK,2,UZ,disp2z

LSWRITE,step
*ENDDO

LSSOLVE,1,OPlanar_angle

FINISH                          ! Finish the solution processor

!****************************************
!*********** Postprocessor ***************
!****************************************
/POST1                          ! Enter the postprocessor

*DIM,OPlanar,TABLE,OPlanar_angle,6
*DIM,Planar,TABLE,OPlanar_angle,6
*DIM,Arc,TABLE,OPlanar_angle,6

*Do,i,1,OPlanar_angle
SET,i                           ! Read data for step "i"
*GET,fx1,Node,nkp2,RF,FX        ! Assign Ortho-planar data to
                                ! OPlanar table
*SET,OPlanar(i,1),fx1
*GET,fy1,Node,nkp2,RF,FY
*SET,OPlanar(i,2),fy1
*GET,fz1,Node,nkp2,RF,FZ
*SET,OPlanar(i,3),fz1
*GET,mx1,Node,nkp2,RF,MX
*SET,OPlanar(i,4),mx1
*GET,my1,Node,nkp2,RF,MY
*SET,OPlanar(i,5),my1
*GET,mz1,Node,nkp2,RF,MZ
*SET,OPlanar(i,6),mz1

*GET,x1,Node,nkp3,U,X           ! Assign planar data to Planar
                                ! table
*SET,Planar(i,1),x1
*GET,y1,Node,nkp3,U,Y
*SET,Planar(i,2),y1
```

Appendix B (Continued)

```
*GET,z1,Node,nkp3,U,Z
*SET,Planar(i,3),z1
*GET,fx1,Node,nkp3,RF,FX
*SET,Planar(i,4),fx1
*GET,fy1,Node,nkp3,RF,FY
*SET,Planar(i,5),fy1
*GET,fz1,Node,nkp3,RF,FZ
*SET,Planar(i,6),fz1

*GET,x1,Node,nkp4,U,X          ! Assign arc data & moment of
                               ! origin to Arc table
*SET,Arc(i,1),x1
*GET,y1,Node,nkp4,U,Y
*SET,Arc(i,2),y1
*GET,z1,Node,nkp4,U,Z
*SET,Arc(i,3),z1
*GET,mx1,Node,nkp1,RF,MX
*SET,Arc(i,4),mx1
*GET,my1,Node,nkp1,RF,MY
*SET,Arc(i,5),my1
*GET,mz1,Node,nkp1,RF,MZ
*SET,Arc(i,6),mz1


*ENDDO

*IF,WRITE,EQ,1,THEN
*cfopen,E:\Thesis\ANSYS\Results\QBM_Unrestrained_data,text

*vwrite,month,'-',day,'-',year,hour,':',minute
%I %C %I %C %I %4.2I %C %2.2I

*vwrite,'Planar:'
%/ %-17C

*vwrite,'Planar-X','Planar-Y','Planar-Z','FX','FY','FZ'
%-17C %-17C %-17C %-16C %-16C %-16C


*vwrite,Planar(1,1),Planar(1,2),Planar(1,3),Planar(1,4),Planar(1,
5),Planar(1,6)
%16.8G %16.8G %16.8G %16.8G %16.8G %16.8G


*vwrite,'Arc displacement & Moments at origin:'
%/ %/ %C
```

Appendix B (Continued)

```
*vwrite,'Arc-X','Arc-Y','Arc-Z','O-MX','O-MY','O-MZ'
%-17C %-17C %-17C %-16C %-16C %-16C

*vwrite,Arc(1,1),Arc(1,2),Arc(1,3),Arc(1,4),Arc(1,5),Arc(1,6)
%16.8G %16.8G %16.8G %16.8G %16.8G %16.8G

*vwrite,'Ortho-Planar:'
%/ %/%-17C

*vwrite,'FX','FY','FZ','MX','MY','MZ'
%-17C %-17C %-17C %-16C %-16C %-16C


*vwrite,OPlanar(1,1),OPlanar(1,2),OPlanar(1,3),OPlanar(1,4),OPlan
ar(1,5),OPlanar(1,6)
%16.8G %16.8G %16.8G %16.8G %16.8G %16.8G

*cfclose
*ENDIF


PLDISP,1                        ! Displays deformed & undeformed
                                ! shape
/VIEW,1,1                       ! Switches to right view
/ANG,1,-90,ZS,0                 ! Rotates View
/ANG,1,15,XS,1                  ! Rotates View

SET,LAST
/REPLOT
/FOC,1,AUTO,,,1
/FOC,1,-0.5,-0.05,,1
/REPLOT

ANTIME,45,0.1, ,1,1,0,0         ! Animate
```

Appendix C: MATLAB Code for a Restrained QBM

```
% MATLAB analysis of restrained ANSYS FEA data
clear all

for Theta= 0:5:90;
Phi      = 5;
Radius   = 100;

% **************Import ANSYS Data***************
if (Theta < 10)
filename = sprintf('QBM_Data_Theta=%01d.text',Theta);
else
filename = sprintf('QBM_Data_Theta=%02d.text',Theta);
end

fileloc  = 'J:\Thesis\ANSYS\Results\';
% Files located on flash drive (Check drive letter)
fid      = fopen([fileloc,filename]);
% Opens the file
rawfile  = native2unicode(fread(fid))';
% Reads file as machine code & changes data to text
fclose(fid);
% Closes the data file

Pointer1 = findstr('MZ', rawfile);
% Finds end of first row of header titles
Pointer2 = findstr('Ortho-Planar',rawfile);
% Finds start of second data set

Pdata    = str2num(rawfile(Pointer1(1)+3:Pointer2(2)-1));
OPdata   = str2num(rawfile(Pointer1(2)+3:end));

% **************Define Rotations****************
OP_rot   = [-[1:Theta]*pi/180,-Theta*pi/180*ones([1 2*Phi])];
P_rot    = [0*ones([1 Theta]),[.5:.5:Phi]*pi/180];

for i = 1:length(OP_rot)
    theta_step = OP_rot(i);
    phi_step   = P_rot(i);

    % Rotation Matrices
    B = [1 0 0; 0 cos(theta_step) sin(theta_step); 0 -
sin(theta_step) cos(theta_step)];
    A = [cos(phi_step) sin(phi_step) 0; -sin(phi_step)
cos(phi_step) 0; 0 0 1];

    OP_F_o      = OPdata(i,1:3)';
    % OP Force matrix in X,Y,Z frame
    OP_M_o      = OPdata(i,4:6)';
```

Appendix C (Continued)

```
    % OP Moments matrix in X,Y,Z frame
    P_F_o       = Pdata(i,1:3)';
    % Planar Force matrix in X,Y,Z frame
    P_M_o       = Pdata(i,4:6)';
    % Planar Moments matrix in X,Y,Z frame
    OP_F_b(i,:) = (B*OP_F_o)';
    % OP Force matrix in B frame
    OP_M_b(i,:) = (B*OP_M_o)';
    % OP Moment matrix in B frame
    P_F_a(i,:)  = (A*P_F_o)';
    % Planar Force matrix in A frame
    P_M_a(i,:)  = (A*P_M_o)';
    % Planar Moment matrix in A frame
    S_OP_M(i,:) = OP_M_o(1,1) - Radius*OP_F_b(i,3);
    % Total Moment about X for the OP link
    S_P_M(i,:)  = P_M_o(3,1) + Radius*P_F_a(i,2);
    % Total Moment about Z for the P link
end

% **************Plots & Figures*****************

set(0,'DefaultAxesColorOrder',[0.6,0.6,0.6])

figure(1)
hold on
order    = 4;
% Order of polynomial fit
[p,S]    = polyfit(P_rot(Theta+1:end)'*180/pi,
S_OP_M(Theta+1:end,1),order);
[y,delta]= polyval(p,P_rot(Theta+1:end)'*180/pi,S);
max_delta= max(delta);

poly_roots = roots(p);
[i,j,v]    = find(imag(poly_roots)==0);
real_roots = poly_roots(i);
[i,j,v]    = find(real_roots>0);
positive_roots = real_roots(i);
good_zero  = min(positive_roots);

plot(P_rot(Theta+1:end)*180/pi,S_OP_M(Theta+1:end,1),'*k')
plot(P_rot(Theta+1:end)'*180/pi,y,'k',P_rot(Theta+1:end)'*180/pi,
y+delta,P_rot(Theta+1:end)'*180/pi,y-delta)

xlabel('Phi','FontSize',12)
ylabel('Mx of OP link','FontSize',12)
title('\it{Phi vs. OP Moment}','FontSize',16)
```

Appendix C (Continued)

```
figure(2)
hold on
[p,S]    = polyfit(P_rot(Theta+1:end)'*180/pi,
P_F_a(Theta+1:end,2),order);
[y,delta]= polyval(p,P_rot(Theta+1:end)'*180/pi,S);

plot(P_rot(Theta+1:end)*180/pi,P_F_a(Theta+1:end,2),'*k')
plot(P_rot(Theta+1:end)*180/pi,y,'k',P_rot(Theta+1:end)*180/pi,y+
delta,P_rot(Theta+1:end)*180/pi,y-delta)

xlabel('Phi','FontSize',12)
ylabel('Planar Force','FontSize',12)
title('\it{Phi vs. Planar Force}','FontSize',16)

if (Theta > 0)
[P_force(Theta/5,:),P_delta] = polyval(p,good_zero,S);
end


figure(3)
clf
hold on
plot3([0,1],[0,0],[0,0])
plot3([0,0],[0,-1],[0,0])
plot3([0,cos(Phi*pi/180)],[0,sin(Phi*pi/180)],[0,0],'k')
plot3([0,0],[0,-cos(Theta*pi/180)],[0,sin(Theta*pi/180)],'k')

x1 = [cos(P_rot(Theta+1:end)),zeros(size([1:2*Phi]))];
y1 = [sin(P_rot(Theta+1:end)),-
cos(Theta*pi/180)*ones(size([1:2*Phi]))];
z1 =
[zeros(size([1:2*Phi])),sin(Theta*pi/180)*ones(size([1:2*Phi]))];
u1 = [Pdata(Theta+1:Theta + 2* Phi,1),OPdata(Theta+1:Theta + 2*
Phi,1)];
v1 = [Pdata(Theta+1:Theta + 2* Phi,2),OPdata(Theta+1:Theta + 2*
Phi,2)];
w1 = [Pdata(Theta+1:Theta + 2* Phi,3),OPdata(Theta+1:Theta + 2*
Phi,3)];

quiver3(x1,y1,z1,-u1,-v1,-w1,5,'r')
view(3)

xlabel('X','FontSize',12)
ylabel('Y','FontSize',12)
zlabel('Z','FontSize',12)
title('\it{Force Vectors on Links}','FontSize',16)
```

Appendix C (Continued)

```
axis equal
grid on


figure(4)
hold on

Px = [Radius*cos(P_rot(Theta+1:end))];
Py = [Radius*sin(P_rot(Theta+1:end))];
Pz = [zeros(size([1:2*Phi]))];

OPx = [zeros(size([1:2*Phi]))];
OPy = [Radius*-cos(Theta*pi/180)*ones(size([1:2*Phi]))];
OPz = [Radius*sin(Theta*pi/180)*ones(size([1:2*Phi]))];

Dist_AB = sqrt((OPx-Px).^2+(OPy-Py).^2+(OPz-Pz).^2);
D_init = Radius * sqrt(2);

D_change = Dist_AB - D_init;

OPFx = [OPdata(Theta+1:Theta + 2* Phi,1)];
OPFy = [OPdata(Theta+1:Theta + 2* Phi,2)];
OPFz = [OPdata(Theta+1:Theta + 2* Phi,3)];

OPF_mag = sqrt(OPFx.^2 + OPFy.^2 + OPFz.^2);

PFx = [Pdata(Theta+1:Theta + 2* Phi,1)];
PFy = [Pdata(Theta+1:Theta + 2* Phi,2)];
PFz = [Pdata(Theta+1:Theta + 2* Phi,3)];

PF_mag = sqrt(PFx.^2 + PFy.^2 + PFz.^2);

Avg_F = (OPF_mag + PF_mag)/2;

K = Avg_F./ D_change';

plot(D_change,Avg_F,'-*k')

xlabel('Change in Length','FontSize',12)
ylabel('Force','FontSize',12)
title('\it{Change in Length vs. Force}','FontSize',16)
```

Appendix C (Continued)

```
figure(5)
hold on

Phi_change = P_rot(Theta+1:end)*180/pi;
plot(Phi_change,S_P_M(Theta+1:end),'-*k')

xlabel('Phi','FontSize',12)
ylabel('Mz of P link','FontSize',12)
title('\it{Phi vs. Planar Moment}','FontSize',16)

%pause
end


figure(6)
hold on
[p,S]    = polyfit([5:5:Theta]',P_force(1:end),order);
[y,delta]= polyval(p,[5:5:Theta]',S);
max(delta)

plot([5:5:Theta],P_force(1:end),'dk')
plot([5:5:Theta]',y,'k',[5:5:Theta]',y+delta,[5:5:Theta]',y-
delta)

xlabel('Out-of-plane angle, \theta','FontSize',12)
ylabel('Planar Threshold Force ( \mu N)','FontSize',12)
title('\it{Theta vs. Planar Threshold Force}','FontSize',16)
```

Appendix D: MATLAB Code for an Unrestrained QBM

```
% MATLAB analysis of unrestrained ANSYS FEA data
clear all

Theta    = 90;
Radius   = 100;

% **************Import ANSYS Data***************

filename = 'QBM_Unrestrained_data.text';
fileloc  = 'J:\Thesis\ANSYS\Results\';
% Files located on flash drive (Check drive letter)
fid      = fopen([fileloc,filename]);
% Opens the file
rawfile  = native2unicode(fread(fid))';
% Reads file as machine code & changes data to text
fclose(fid);
% Closes the data file

Pointer1 = findstr('FZ', rawfile);
% Finds end of first row of header titles
Pointer2 = findstr('Arc position',rawfile);
% Finds start of second data set
Pointer3 = findstr('MZ',rawfile);
% Finds end of second & third row of header titles
Pointer4 = findstr('Ortho-Planar',rawfile);
% Finds start of third data set

Pdata    = str2num(rawfile(Pointer1(1)+3:Pointer2(1)-1));
Arc_Origin_data    = str2num(rawfile(Pointer3(1)+3:Pointer4(1)-
1));
OPdata   = str2num(rawfile(Pointer3(2)+3:end));

% **************Define Rotations****************

OP_Loc   = [zeros([1 Theta]);-
Radius*cos([1:Theta]*pi/180);Radius*sin([1:Theta]*pi/180)]';

for i = 1:1:Theta

    % Rotation Matrix for OP link
    B = [1 0 0; 0 cos(i*pi/180) sin(i*pi/180); 0 -sin(i*pi/180)
cos(i*pi/180)];

    P_Loc(i,:)   = ([Radius,0,0] + Pdata(i,1:3))';
    % Planar Location matrix in X,Y,Z frame
    P_F(i,:)   = Pdata(i,4:6)';
    % Planar Force matrix in X,Y,Z frame

    Arc_Loc(i,:) = ([Radius*cos(45*pi/180),-
Radius*sin(45*pi/180),0] + Arc_Origin_data(i,1:3))';
    Origin_M(i,:)= Arc_Origin_data(i,4:6)';
    % Moments at the origin matrix in X,Y,Z frame
```

Appendix D (Continued)

```
    OP_F(i,:) = OPdata(i,1:3)';
    % OP Force matrix in X,Y,Z frame
    OP_M(i,:) = OPdata(i,4:6)';
    % OP Moments matrix in X,Y,Z frame

    % ****compare with Alex's model*****
    OP_F_B(i,:) = B*OPdata(i,1:3)';
    % OP Force matrix in B-frame
    OP_M_B(i,:) = B*OPdata(i,4:6)';
    % OP Moments matrix in B-frame

    Arc_angle_s=atan2(Arc_Loc(i,2),Arc_Loc(i,1))*180/pi;
    C(i,:,:) = [cos(Arc_angle_s) sin(Arc_angle_s) 0; -
sin(Arc_angle_s) cos(Arc_angle_s) 0; 0 0 1];

end

% **************Plots & Figures*****************
set(0,'DefaultAxesColorOrder',[0.6,0.6,0.6])

figure(1)
clf

Dis1 = P_Loc  - Arc_Loc;
Dis2 = OP_Loc - Arc_Loc;

D1= sqrt(Dis1(:,1).^2+Dis1(:,2).^2+Dis1(:,3).^2);
D2= sqrt(Dis2(:,1).^2+Dis2(:,2).^2+Dis2(:,3).^2);

plot([1:Theta],D1,'-*k',[1:Theta],D2,'-*g')

xlabel('Theta','FontSize',12)
ylabel('Distance to Arc Center','FontSize',12)
title('\it{Distance to Arc Center}','FontSize',16)
legend('Planar link','OP link','Location','SouthWest')


figure(2)
clf
plot([1:Theta],D1-D2,'*k')

xlabel('Theta','FontSize',12)
ylabel('Change in Distance','FontSize',12)
title('\it{Change in Distance}','FontSize',16)


figure(3)
clf

PR   =sqrt(P_Loc(:,1).^2+P_Loc(:,2).^2+P_Loc(:,3).^2);
OPR  =sqrt(OP_Loc(:,1).^2+OP_Loc(:,2).^2+OP_Loc(:,3).^2);
ArcR =sqrt(Arc_Loc(:,1).^2+Arc_Loc(:,2).^2+Arc_Loc(:,3).^2);

plot([1:Theta],PR,'b',[1:Theta],OPR,'r',[1:Theta],ArcR,'g')
```

Appendix D (Continued)

```
xlabel('Theta','FontSize',12)
ylabel('Radial Distance','FontSize',12)
title('\it{Radial Distance}','FontSize',16)
legend('Planar link','OP link','Arc
Center','Location','SouthWest')


figure(4)
clf

Arc_angle1=atan2(Arc_Loc(:,2),Arc_Loc(:,1))*180/pi;
Arc_angle2=atan2(Arc_Loc(:,3),sqrt(Arc_Loc(:,1).^2+Arc_Loc(:,2).^
2))*180/pi;

P_angle1=atan2(P_Loc(:,2),P_Loc(:,1));
P_angle2=atan2(P_Loc(:,3),sqrt(P_Loc(:,1).^2+P_Loc(:,2).^2));

OP_angle1=atan2(OP_Loc(:,2),OP_Loc(:,1));
OP_angle2=atan2(OP_Loc(:,3),sqrt(OP_Loc(:,1).^2+OP_Loc(:,2).^2));

Ang1 = (OP_angle1+P_angle1)/2*180/pi;
Ang2 = (OP_angle2+P_angle2)/2*180/pi;

plot([1:Theta],Arc_angle1,'-*g',[1:Theta],Ang1,'-*b')


figure(5)
clf
plot([1:Theta],Arc_angle2,'-*g',[1:Theta],Ang2,'-*b')
% The green line is significant only because it shows the inward
% sagging of the compliant link, due in part to tensile forces.
% It also shows a violation of the assumption of Alex/Saurabh's
% model, though not a large one.


figure(6)
clf
hold on

quiver3(OP_Loc(:,1),OP_Loc(:,2),OP_Loc(:,3),OP_F(:,1),OP_F(:,2),O
P_F(:,3))
quiver3(OP_Loc(:,1),OP_Loc(:,2),OP_Loc(:,3),OP_M(:,1),OP_M(:,2),O
P_M(:,3),'k')

OP_M_mag = (OP_M(:,1).^2+OP_M(:,2).^2+OP_M(:,3).^2).^0.5;
OP_F_mag = (OP_F(:,1).^2+OP_F(:,2).^2+OP_F(:,3).^2).^0.5;
OP_F_unit = OP_F./(OP_F_mag*[1 1 1]);
M_par_mag = dot(OP_F_unit',OP_M')'*[1 1 1];
M_par = M_par_mag.*OP_F_unit;
M_perp = OP_M - M_par;
M_perp_mag = (M_perp(:,1).^2+M_perp(:,2).^2+M_perp(:,3).^2).^0.5;
M_perp_unit = M_perp./(M_perp_mag*[1 1 1]);
d_unit = -cross(OP_F_unit',M_perp_unit')';
d_mag1 = M_perp_mag./OP_F_mag;
d1 = (d_mag1*[1 1 1]).*d_unit;
```

Appendix D (Continued)

```
%quiver3(OP_Loc(:,1),OP_Loc(:,2),OP_Loc(:,3),d1(:,1),d1(:,2),d1(:
,3),0,'g')
screwpt1 = OP_Loc+d1;


% center calculations
quiver3(Arc_Loc(:,1),Arc_Loc(:,2),Arc_Loc(:,3),OP_F(:,1),OP_F(:,2
),OP_F(:,3),'b')

M_center = cross(-Dis2,OP_F)+OP_M;
quiver3(Arc_Loc(:,1),Arc_Loc(:,2),Arc_Loc(:,3),M_center(:,1),M_ce
nter(:,2),M_center(:,3),'g')

M_C= (squeeze(C(i,:,:))*M_center')';
F_C= (squeeze(C(i,:,:))*OPdata(:,1:3)')';

M_center_mag =
(M_center(:,1).^2+M_center(:,2).^2+M_center(:,3).^2).^0.5;

%OP_F_mag = (OP_F(:,1).^2+OP_F(:,2).^2+OP_F(:,3).^2).^0.5;
%OP_F_unit = OP_F./(OP_F_mag*[1 1 1]);
M_center_par_mag = dot(OP_F_unit',M_center')'*[1 1 1];
M_center_par = M_center_par_mag.*OP_F_unit;
M_center_perp = M_center - M_center_par;
M_center_perp_mag =
(M_center_perp(:,1).^2+M_center_perp(:,2).^2+M_center_perp(:,3).^
2).^0.5;
M_center_perp_unit = M_center_perp./(M_center_perp_mag*[1 1 1]);
d_unit2 = -cross(OP_F_unit',M_center_perp_unit')';
d_mag2 = M_center_perp_mag./OP_F_mag;
d2 = (d_mag2*[1 1 1]).*d_unit2;
%quiver3(Arc_Loc(:,1),Arc_Loc(:,2),Arc_Loc(:,3),d2(:,1),d2(:,2),d
2(:,3),0,'g' )
screwpt2 = Arc_Loc+d2;

screw_axis = screwpt2-screwpt1;

check = cross(screw_axis',OP_F')';
quiver3(screwpt1(:,1),screwpt1(:,2),screwpt1(:,3),screw_axis(:,1)
,screw_axis(:,2),screw_axis(:,3),0,'r')

%plot([1:Theta],M_center,'-*')

xlabel('X','FontSize',12)
ylabel('Y','FontSize',12)
zlabel('Z','FontSize',12)
title('\it{Equivalent Screwpoint of Arc Center}','FontSize',16)
legend('OP Forces','OP Moments','Arc Center Forces','Arc Center
Moments','Screwpoint','Location','Best')

grid on
view(38,27)
```

Appendix D (Continued)

```
% **************Half PRBM**********************
% Leon PRBM: Use two 45 degree models
% Asp  = height/width = 2/5 = 0.4
Beta  = [0.5:.5:45]'*pi/180;
%lambda = 45*pi/180*(1+2*[.1:.45]);
% possible change in lambda due to elongation
lambda  = 45*pi/180;
gamma = 0.846;
%gamma = 1.25;
c_theta = 1.21;
% parametric angle coefficient
K_f   = 1.9;
K_m   = 0.2;
Cap_Theta = asin(sin(Beta)/sin(gamma*lambda));
flag1 = 1-abs(sign(imag(Cap_Theta)));
Cap_Theta = Cap_Theta./flag1;
Phi   = atan2(1-
cos(Cap_Theta),cot(gamma*lambda)+cos(Cap_Theta)*tan(gamma*lambda)
);
Alpha = pi/4-Phi;

h=2;
b=5;
E=170000;
I=1/12*b*h*h*h;
DTB=cos(Cap_Theta).*sin(gamma*lambda)./cos(Beta);
F_model = K_f*(E*I/(lambda*Radius^2))*Cap_Theta.*DTB;
M_model = K_m*(E*I/(lambda*Radius))*Cap_Theta.*DTB;


figure(4)
% add to figure 4
hold on
plot(2*Beta*180/pi,-45-Phi*180/pi,'yo-')

xlabel('OP Angle, \theta','FontSize',12)
ylabel('Planar Angle of Arc Center','FontSize',12)
title('\it{Planar Angles of the Arc Center}','FontSize',16)
legend('Planar angle of arc center','Average planar angle of P &
OP links','Planar angle of Half PRBM','Location','SouthWest')
```

Appendix D (Continued)

```
figure(5)
% add to figure 5
hold on
plot(2*Beta*180/pi,Beta*180/pi,'yo-')

xlabel('OP Angle, \theta','FontSize',12)
ylabel('OP Angle of Arc Center','FontSize',12)
title('\it{Ortho-Planar Angles of the Arc Center}','FontSize',16)
legend('OP angle of arc center','Average OP angle of P & OP
links','OP angle of Half PRBM','Location','SouthEast')


figure(7)
clf
hold on
plot(2*Beta*180/pi,F_C(:,3),'b*-')
plot(2*Beta*180/pi,F_model,'k*-')

xlabel('Theta','FontSize',12)
ylabel('Force','FontSize',12)
title('\it{Forces}','FontSize',16)
legend('Actual','Predicted by model','Location','Best')


figure(8)
clf
hold on
plot(2*Beta*180/pi,M_C(:,2),'b*-')
plot(2*Beta*180/pi,M_model,'k*-')

xlabel('Theta','FontSize',12)
ylabel('Moment','FontSize',12)
title('\it{Moments}','FontSize',16)
legend('Actual','Predicted by model','Location','Best')

figure(9)
clf
hold on
plot(2*Beta*180/pi,M_C(:,2)./F_C(:,3),'b*-')
plot(2*Beta*180/pi,M_model./F_model,'k*-')

xlabel('Theta','FontSize',12)
ylabel('Moment/Force','FontSize',12)
title('\it{Ratio of Moments/Forces}','FontSize',16)
legend('Actual','Predicted by model','Location','Best')
```

Appendix E: ANSYS Code for the BAP

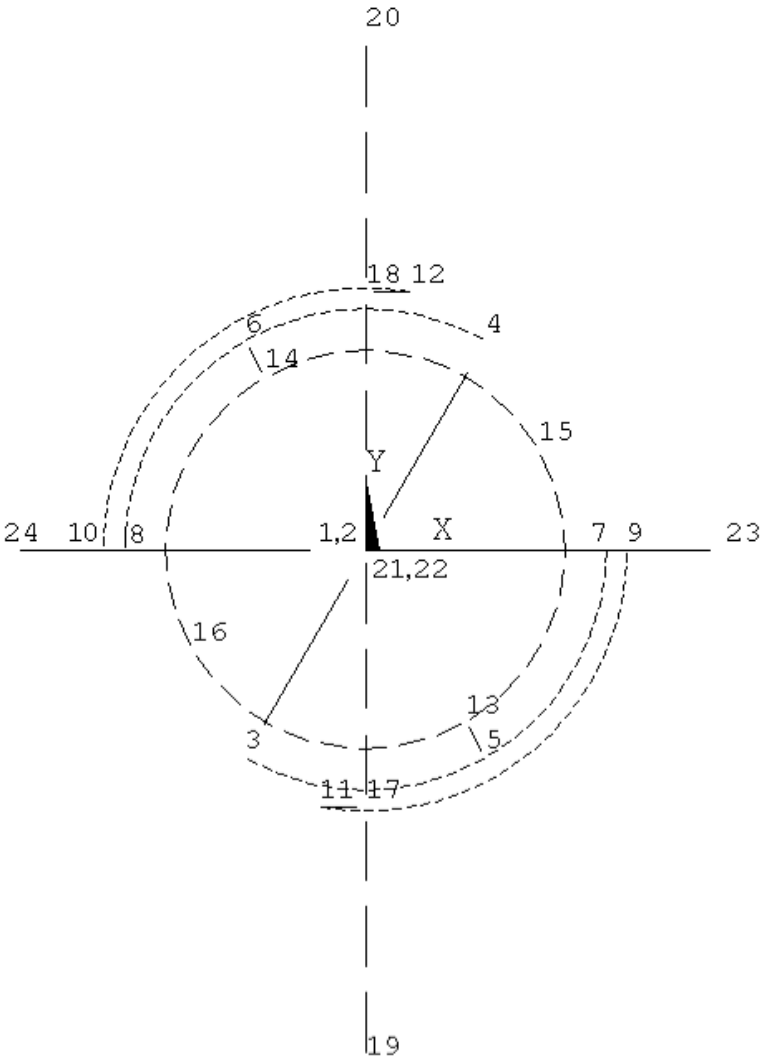

Figure E.1 ANSYS Model of the BAP

```
!*****************************************************************
!/CWD,'J:\Thesis\ANSYS'
!*****************************************************************

FINISH
/CLEAR

/FILNAM,Bistable Aerial Platform
/title,Bistable Aerial Platform

/PREP7                          ! Enter the pre-processor
```

Appendix E (Continued)

```
!****************************************
!********** Model Parameters ************
!****************************************

PI=acos(-1.)

R1=76                          ! Radius of elevating ring
R2=91.5                        ! Radius of input link
                               ! (aka actuator)
R3=99.5                        ! Radius of bistable element
R4=137                         ! Radius of guide ring
L=196                          ! Total length of ortho-planar beam

phi= -120*PI/180               ! Initial angle of position for the
input link
psi= 260*PI/180                ! Initial angle to define the
                               ! connection between ortho-planar
                               ! beam and bistable element

h1=2                           ! Thickness of Poly1
h2=1.5                         ! Thickness of Poly2

b1=42                          ! Width of ortho-planar beam
b2=10                          ! Width of remaining beam elements
b3=20                          ! Width of elevating ring
b4=5                           ! Width of compliant segments
                               ! (actuator and bistable element)

!************ Define Area ***************

A1 = h2*b1                     ! Cross sectional area of the
                               ! ortho-planar beam
Iz1= 1/12*b1*h2*h2*h2          ! Second Moment of Area
                               ! (aka Area Moment of Inertia)
Ix1= 1/12*h2*b1*b1*b1

A2=  h1*b2                     ! Cross sectional of the remaining
                               ! beam elements
Iz2= 1/12*b2*h1*h1*h1
Ix2= 1/12*h1*b2*b2*b2

A3=  h1*b3                     ! Cross sectional area of the
                               ! elevating ring
Iz3= 1/12*b3*h1*h1*h1
Ix3= 1/12*h1*b3*b3*b3

A4=  h1*b4                     ! Cross sectional area of the
                               ! compliant segments
```

Appendix E (Continued)

```
Iz4= 1/12*b4*h1*h1*h1
Ix4= 1/12*h1*b4*b4*b4


!*****************************************
!********** Define Keypoints *************
!*****************************************

! Create Keypoints: K(Point #, X-Coord, Y-Coord, Z-Coord)

! Point of rotation for ortho-planar link
K,1,0,0,h1+h2/2,
K,2,0,0,h1+h2/2,

! Actuation points
K,3,R2*cos(phi),R2*sin(phi),0,
K,4,R2*cos(phi+PI),R2*sin(phi+PI),0,

! Center of actuator link
K,5,R2*cos(phi/2),R2*sin(phi/2),h1*2,
K,6,-R2*cos(phi/2),-R2*sin(phi/2),h1*2,

! Rotating beams
K,7,R2,0,0,
K,8,-R2,0,0,
K,9,R3,0,0,
K,10,-R3,0,0,

! Point of connection between the ortho-planar link and the
! quadrantal beam
K,11,R3*cos(psi),R3*sin(psi),h1+h2/2,
K,12,-R3*cos(psi),-R3*sin(psi),h1+h2/2,

! Elevating Ring
K,13,R1*cos(phi/2),R1*sin(phi/2),0,
K,14,-R1*cos(phi/2),-R1*sin(phi/2),0,
K,15,R1*cos(phi/2+PI/2),R1*sin(phi/2+PI/2),0,
K,16,R1*cos(phi/2-PI/2),R1*sin(phi/2-PI/2),0,

! Points on ortho-planar link
K,17,0,R3*sin(psi),h1+h2/2,
K,18,0,-R3*sin(psi),h1+h2/2,
K,19,0,-L,h1,
K,20,0,L,h1,
```

Appendix E (Continued)

```
! Additional points at origin
K,21,0,0,0,
K,22,0,0,0,

! Guide "Ring"
K,23,R4,0,0,
K,24,-R4,0,0


!*****************************************
!************ Create Links ***************
!*****************************************

!*********** Straight links **************

! Ortho-planar links
LSTR,       1,       17       ! #1
LSTR,       2,       18       ! #2
LSTR,       17,      11       ! #3
LSTR,       18,      12       ! #4
LSTR,       17,      19       ! #5
LSTR,       18,      20       ! #6

! Beam connecting actuations points
LSTR,       3,       21       ! #7
LSTR,       21,      4        ! #8

! Rotating Beams
LSTR,       7,       9        ! #9
LSTR,       8,       10       ! #10
LSTR,       22,      23       ! #11
LSTR,       22,      24       ! #12
LSTR,       23,      9        ! #13
LSTR,       24,      10       ! #14

! Beam attaching center of actuator arc to elevating ring
LSTR,       5,       13       ! #15
LSTR,       6,       14       ! #16

LESIZE,ALL,,,1                ! Specifies a single division on
                              ! unmeshed lines

LESIZE,1,,,3
LESIZE,2,,,3
LESIZE,5,,,3
LESIZE,6,,,3
```

Appendix E (Continued)

```
!************** Arc links ****************
! Elevating ring
LARC,16,13,21,R1,              ! #17
LARC,14,16,21,R1,              ! #18
LARC,15,13,21,R1,              ! #19
LARC,14,15,21,R1,              ! #20

! Actuator
LARC,3,5,21,R2,                ! #21 *Compliant*
LARC,5,7,21,R2,                ! #22 *Compliant*
LARC,4,6,21,R2,                ! #23 *Compliant*
LARC,6,8,21,R2,                ! #24 *Compliant*

! Quadrantal Beam
LARC,9,11,21,R3,               ! #25 *Compliant*
LARC,10,12,21,R3,              ! #26 *Compliant*

! Guide Ring
!LARC,23,24,22,R4,              ! #27
!LARC,24,25,22,R4,              ! #28
!LARC,25,26,22,R4,              ! #29
!LARC,26,23,22,R4,              ! #30

LSEL,S,,,17,20                 ! Divides the rigid arcs into 8
segments
!LSEL,A,,,27,30
LESIZE,ALL,,,8

LSEL,S,,,21,24                 ! Actuator divided into two parts
with 16 segments each
LESIZE,ALL,,,16

LSEL,S,,,25,26                 ! Divides the compliant arcs of the
                               ! quadrantal beams into 32 segments
LESIZE,ALL,,,32

LSEL,ALL

!******** Declare element type  **********
ET,1,BEAM4
KEYOPT,1,2,1
KEYOPT,1,6,1

!******** Define Real Constants *********
R,1,A1,Ix1,Iz1,h2,b1, ,      ! Properties of ortho-planar beam
R,2,A2,Ix2,Iz2,h1,b2, ,      ! Properties of other beam elements
R,3,A3,Ix3,Iz3,h1,b3, ,      ! Properties of elevating ring
R,4,A3,Ix4,Iz4,h1,b4, ,      ! Properties of compliant segments
```

Appendix E (Continued)

```
!****** Define Material Properties ******
MP,EX,1,170000                ! Young's Modulus of Elasticity
                              ! (MPa)
MP,PRXY,1,0.22                ! Poisson's ratio

!*****************************************
!*************** Mesh ******************
!*****************************************

type,1                         ! Use element type 1
mat,1                          ! Use material property set 1

real,1                         ! Use real constant set 1
LMESH,1,8                      ! Mesh lines 1-8
!LMESH,27,30                    ! Mesh lines 27-30

real,2                         ! Use real constant set 2
LMESH,9,16                     ! mesh lines 9-16

real,3                         ! Use real constant set 3
LMESH,17,20                    ! Mesh lines 17-20

real,4                         ! Use real constant set 4
LMESH,21,26                    ! Mesh lines 21-26


!*****************************************
!******** Create Contact Elements ********
!*****************************************

ET,2,Targe170
ET,3,Conta176
KEYOPT,3,2,1                   ! Use penalty function contact
                               ! algorithms
KEYOPT,3,3,1                   ! Specify crossing beams
KEYOPT,3,5,3                   ! Reduce gap/penetration with
                               ! auto CNOF
KEYOPT,3,6,1                   ! Allow nominal refinement to
contact stiffness
KEYOPT,3,7,3                   ! Allow change in the contact
                               ! predictions
KEYOPT,3,10,1                  ! Update contact stiffness after
each substep
```

Appendix E (Continued)

```
R,5,h2/2,h1/2,0.25
R,6,h2/2,h1/2,0.25
REAL,5

! Generate the target surface
LSEL,S,,,1
LSEL,A,,,5
TYPE,2
NSLL,S,1
ESLL,S,0
ESURF
ESURF,,REVE

! Generate the contact surface
LSEL,S,,,17,18
TYPE,3
NSLL,S,1
ESLL,S,0
ESURF,,BOTTOM

REAL,6

! Generate the target surface
LSEL,S,,,2
LSEL,A,,,6
TYPE,2
NSLL,S,1
ESLL,S,0
ESURF
ESURF,,REVE

! Generate the contact surface
LSEL,S,,,19,20
TYPE,3
NSLL,S,1
ESLL,S,0
ESURF,,TOP

ALLSEL

!*****************************************
!******** Get Node # of Keypoints ********
!*****************************************

ksel,s,kp,,3
nslk,s
*get,nkp3,node,0,num,max
```

Appendix E (Continued)

```
ksel,s,kp,,4
nslk,s
*get,nkp4,node,0,num,max

ksel,s,kp,,5
nslk,s
*get,nkp5,node,0,num,max

ksel,s,kp,,6
nslk,s
*get,nkp6,node,0,num,max

ksel,s,kp,,7
nslk,s
*get,nkp7,node,0,num,max

ksel,s,kp,,8
nslk,s
*get,nkp8,node,0,num,max

ksel,s,kp,,11
nslk,s
*get,nkp11,node,0,num,max

ksel,s,kp,,12
nslk,s
*get,nkp12,node,0,num,max

ksel,s,kp,,22
nslk,s
*get,nkp22,node,0,num,max

ALLSEL
FINISH                          ! Finish pre-processing

!*****************************************
!************* Solution ******************
!*****************************************

KEYW,PR_SGUI,1                  ! Suppresses "Solution is Done"
                                ! text box
/SOL                            ! Enter the solution processor
/gst,off                        ! Turn off the graphical
                                ! convergence monitor
```

Appendix E (Continued)

```
ANTYPE,0                        ! Analysis type, static
NLGEOM,ON                       ! Includes large-deflection effects
                                ! in a static or full transient
                                ! analysis
SOLCONTROL,ON,ON                ! Gives ANSYS control of the time
                                ! step size
LNSRCH,AUTO                     ! ANSYS automatically switches line
                                ! search on/off
NEQIT,100                       ! Set max # of iterations to 100
DELTIM,,0.0001                  ! Set minimum time step increment

!**** Define Displacement Constraints*****

DK,1,,0,,,UX,UY,UZ,ROTY,ROTZ
DK,2,,0,,,UX,UY,UZ,ROTY,ROTZ
DK,3,UZ,0
DK,4,UZ,0
!DK,9,UZ,0
!DK,10,UZ,0

KSEL,S,,,23,24
DK,ALL,,0,,,UZ

KSEL,S,,,13,16
DK,ALL,,0,,,ROTX,ROTY

KSEL,S,,,21,22
DK,ALL,,0,,,UX,UY,UZ,ROTY,ROTX

KSEL,ALL

!********* Displacement Load *************

!ESEL,S,TYPE,,2,3,              ! Select element types 2 & 3,
                                ! which make-up the contact pairs
!EKILL,ALL                      ! Kill all selected elements
!ESEL,ALL                       ! Re-select all elements

CNCHECK,ADJUST                  ! Move contact nodes to close gap
                                ! or reduce penetration

loadsteps=300
*DO,step,1,loadsteps,1
theta=0.25*step*PI/180
DK,21,ROTZ,theta
LSWRITE,step
*ENDDO
```

Appendix E (Continued)

```
!LSSOLVE,1,loadsteps
theta1=ROTZ(nkp22)

LD=loadsteps
*DO,step,1,10,1
DK,22,ROTZ,theta1 + 2*step*PI/180
LSWRITE,LD+step
loadsteps=loadsteps+1
*ENDDO

LSSOLVE,1,loadsteps

KEYW,PR_SGUI,0                ! Undo suppression of "Solution is
                              ! Done" text box
FINISH                        ! Finish the solution processor

!*************************************
!*********** Postprocessor ***************
!*************************************
/POST1                        ! Enter the postprocessor

PLDISP,1                      ! Displays deformed & undeformed
shape
!/VIEW,1,-1                    ! Switches to left view
/VIEW,1,,-1                   ! Switches to bottom view
/ANG,1,30,YS,1                ! Rotates View
/REPLOT,FAST

ANTIME,50,0.05, ,1,1,0,0       ! Animate
```

Appendix F: Coordinate Transformation

The ANSYS data taken provides the forces experienced by the model in terms of the original xyz coordinate system. However, in order to properly monitor the direction of the forces at the ends of the rotating links, a new coordinate system placed at the end of each link is needed. To accomplish this, the forces must be transformed into new frames of reference. The method used to accomplish the transformation is explained below.

F.1. Mathematics of Rotations

A vector **x** is composed of both a parallel component $\mathbf{x}_{\|}$ and a perpendicular component $\mathbf{x}_{\perp}$ with respect to a chosen plane [26].

$$x = x_{\perp} + x_{\|} \tag{F.1}$$

Linearly transforming **x** by applying a rotation about a vector, **A**, which is normal to the plane, will result in

$$x' = x_{\perp} + x_{\|}e^{iA} \tag{F.2}$$

where $\mathbf{x}_{\|}\mathbf{e}^{\mathbf{iA}}$ describes a rotation of $\mathbf{x}_{\|}$ in the plane about **A** and through an angle of magnitude |**A**| [26]. Note that this rotation only affects $\mathbf{x}_{\|}$ and that $\mathbf{x}_{\perp}=\mathbf{x}'_{\perp}$ [26]. The resulting transformation is depicted in Figure F.1.

Appendix F (Continued)

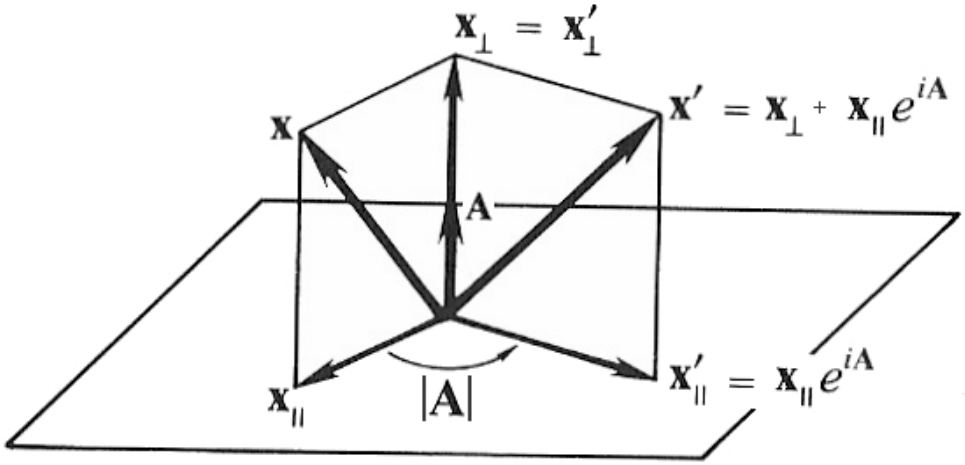

Figure F.1 Rotation of a vector
[26][6]

The rotation, **R**, resulting from the application of $\mathbf{e}^{i\mathbf{A}}$ proves more useful when expressed in the parametric form

$$R = \alpha + i\beta \tag{F.3a}$$

$$= e^{iA}. \tag{F.3b}$$

And since

$$e^{iA} = \cos A + i \sin A \ , \tag{F.4}$$

the parameters $\boldsymbol{\alpha}$, $\boldsymbol{\beta}$, and **A** can be related by

$$\alpha = \cos |A| \tag{F.5}$$

$$\beta = \hat{A} \sin |A| \tag{F.6}$$

where $\hat{\mathbf{A}}$ is a unit vector along the axis of rotation, **A**. In practice, however, a rotation is typically expressed as

[6] Image adapted from Hestenes

Appendix F (Continued)

$$R = R(\sigma,\theta) \tag{F.7}$$

where $\boldsymbol{\sigma}=\hat{\mathbf{A}}$ and $\boldsymbol{\theta}$ represents the magnitude of the rotation, $|\mathbf{A}|$, which indicates that $\mathbf{A}=\boldsymbol{\sigma\theta}$. Thus, equations (F.5) and (F.6) respectively become

$$\alpha = \cos\theta \tag{F.8}$$

$$\beta = \sigma\sin\theta. \tag{F.9}$$

Combining these equations, we arrive at

$$x' = R(\sigma,\theta)x \tag{F.10a}$$
$$= x_{\perp} + x_{\parallel}(e^{i\sigma\theta}) \tag{F.10b}$$
$$= x_{\perp} + x_{\parallel}(\cos\theta + i\sigma\sin\theta)\ , \tag{F.10c}$$

which will be used to develop rotation matrices for the ANSYS model.

F.2. Rotation Matrices

Using the equations developed in the previous section, the data taken from ANSYS can now be transformed from the original frame of reference, O, into new frames, A and B, that rotate with the planar and ortho-planar links, respectively. The original and moving frames are shown below in Figure F.2. Starting with the ortho-

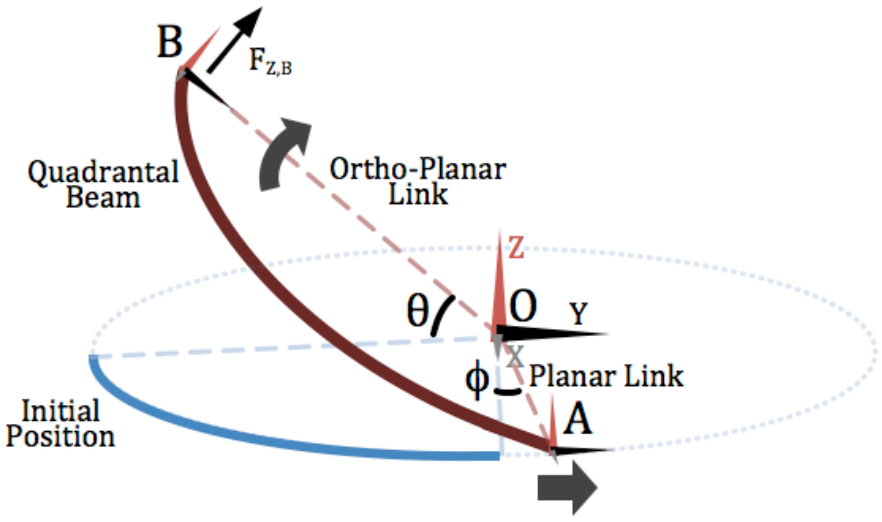

Figure F.2 Rotating frames on the quadrantal beam

planar link and using equation (F.10a), the rotated B-frame becomes

$$\vec{B} = R(O_x, \theta)\vec{O} \tag{F.11}$$

because, as shown in Figure F.2, the B-frame results from a rotation of the original frame about the x-axis by a degree Theta, θ. Likewise, the rotated A-frame represents a rotation about the original z-axis by a degree Phi, ϕ and becomes

$$\vec{A} = R(O_z, \phi)\vec{O}. \tag{F.12}$$

Appendix F (Continued)

Expanding equation (F.11) by using equations (F.10b) for the x-axis results in

$$B_x = R(O_x,\theta)O_x \tag{F.13a}$$
$$= B_\perp + B_\parallel e^{iO_x\theta}. \tag{F.13b}$$

In this instance, since the axis of interest is also the axis of rotation, there is no $B_\parallel$ because O_x is tangent to the plane of rotation. Therefore

$$B_x = O_x. \tag{F.14}$$

Such a simplification results from properly selecting the location and orientation of the new coordinate system; also note that because of this choice, O_y and O_z lie parallel to the plane of rotation for the B-frame.

For y-axis, expanding equation (F.11) by using equations (F.10c) yields

$$B_y = R(O_x,\theta)O_y \tag{F.15a}$$
$$= B_\perp + B_\parallel(\cos\theta + iO_y\sin\theta). \tag{F.15b}$$

Simplifying this equation requires the understanding that

$$i\sigma_x = \sigma_y\sigma_z = \sigma_{yz} \tag{F.16a}$$
$$i\sigma_y = \sigma_x\sigma_z = \sigma_{xz} \tag{F.16b}$$
$$i\sigma_z = \sigma_x\sigma_y = \sigma_{xy}\ , \tag{F.16c}$$

and that

$$\sigma_j\sigma_{jk} = \sigma_k \tag{F.17a}$$
$$\sigma_j\sigma_{kj} = -\sigma_k \tag{F.17b}$$

where both **j** and **k** can represent any one of the three axes. Thus equation (F.15b) becomes

Appendix F (Continued)

$$B_y = B_\perp + B_\parallel(\cos\theta + O_{xz}\sin\theta). \tag{F.18}$$

Since the component of interest, O_y, lies parallel to the plane of rotation for the B-frame as stated before, $B_\perp=0$ and $B_\parallel=O_y$, which will give a final result of

$$B_y = O_y\cos\theta + O_z\sin\theta. \tag{F.19}$$

Similarly, it can be found that

$$B_z = O_z\cos\theta - O_y\sin\theta. \tag{F.20}$$

Combining equations (F.14), (F.19), and (F.20) into a matrix yields

$$\begin{bmatrix} B_x \\ B_y \\ B_z \end{bmatrix} = \begin{bmatrix} 1 & 0 & 0 \\ 0 & \cos\theta & \sin\theta \\ 0 & -\sin\theta & \cos\theta \end{bmatrix} \cdot \begin{bmatrix} O_x \\ O_y \\ O_z \end{bmatrix}, \tag{F.21}$$

which, if viewed as

$$[B] = [R_B]\cdot[O], \tag{F.22}$$

indicates that the original rotation, $R(O_x,\theta)$, applied in (F.11) is equal to

$$[R_B] = \begin{bmatrix} 1 & 0 & 0 \\ 0 & \cos\theta & \sin\theta \\ 0 & -\sin\theta & \cos\theta \end{bmatrix}. \tag{F.23}$$

Applying these same methods to equation (F.12) for the A-frame will show that

$$[A] = [R_A]\cdot[O] \tag{F.24}$$

and that

Appendix F (Continued)

$$[R_A] = \begin{bmatrix} \cos\phi & \sin\phi & 0 \\ -\sin\phi & \cos\phi & 0 \\ 0 & 0 & 1 \end{bmatrix}. \tag{F.25}$$

With equations (F.23) and (F.25) now developed, the force data provided by ANSYS can be adjusted for the planar and ortho-planar links, allowing F_x, F_y, and F_z to be seen in terms of the relative position and orientation of the link.